

1 We would like to thank the editor for his very careful editing and constructive
2 suggestions. In what follows, we make point-by-point responses to the comments
3 and suggestions.

4

5 Please go over this paper very carefully with your co-authors to catch any errors that
6 the suggested changes might introduce.

7 [Response: Our coauthors checked the text carefully and we asked help from Prof. A.
8 David McGuire of University of Alaska Fairbanks to go over the text to prevent
9 grammar errors.](#)

10 Page 4 Ln 16

11 Over a large region, usually monthly CRU data are required because they are the
12 only available, but you say on P6, L19 that the model runs on daily increments. If
13 you were using monthly CRU data to run the model, then you would have to
14 downscale to daily values. But you are not using monthly CRU data, and you are not
15 simulating a region. You are simulating a point, and you have data measured at 30
16 min intervals, and these can be re-sampled to daily values. According to the
17 approach described in this paper, you go from 30 min samples, to monthly averages
18 and then back to daily interpolations used by the DOS-TEM environmental module.
19 You lose an incredible amount of fidelity in the data and it seems absurd.

20

21 Either the model runs on monthly increments and requires monthly data as you
22 suggest on P4, L17, or the model runs on daily increments and requires daily data as
23 you suggest on P6, L19, that can be developed from your 30 min measurements.
24 Which is it?

25

26 This issue must be resolved in a clear manner. I suspect that your results will change
27 if you actually use daily values derived from your 30 min measurements.

28 [Response: Thank you for this comment. The TEM family models use monthly data to drive
29 ecological processes, and use interpolated daily data from monthly data to drive](#)

1 environmental processes. Although 30 min driving data are usually used in land surface
2 models to simulate the exchanges of energy, water, and carbon between land surface and
3 atmosphere, they are seldom used in permafrost or ecosystem models.

4 We agree that the results will change if daily values from 30 min measurement were used
5 directly to drive TEM. Zhuang et al. (2001) performed a test with daily and monthly driving
6 datasets. The results showed that the root mean squared errors of active layer depth were
7 about 3 cm. In our next studies, we plan to apply the model over large regions, where daily
8 driving data might not be available. Therefore, we did not change the code of DOS-TEM to
9 use daily driving data directly. We discuss this uncertainty in Section 4.3.2 as follows:

10

11 The TEM family models use monthly atmospheric data to drive processes in both site and
12 regional applications. In this study, 30 min and daily driving data are available. Although it is
13 possible to lose fidelity after daily interpolations, we decided to use monthly driving data for
14 the following reasons: 1) Zhuang et al. (2001) performed a test with daily and monthly
15 driving datasets, and the results showed that the root mean squared errors of active layer depth
16 were about 3 cm; 2) we plan to apply the model over large regions where reliable daily
17 datasets might not be available.

18

19 Use standard symbols for BD, PORO, and VWC here and throughout the text. For each of
20 these parameters, indicate units here as well (e.g. g cm⁻³). This will help clarify to the reader
21 what parameter you are discussing. E.g. Density is typically indicated by a Greek small letter
22 Rho (ρ). Here you can indicate bulk density by Rho with a “b” subscript, density of water by
23 Rho with a “w” subscript, and particle density by Rho with a “p” subscript.

24 Porosity is often indicated by the Greek small letter Phi (ϕ) and sometimes large letter (e.g.
25 on P7 you use Greek large letter Phi). Here you can indicate measured porosity with an “m”
26 subscript, and porosity derived from bulk density with a “b” subscript.

27 **Response:** Thank you for these suggestions. We changed these symbols as suggested.

28

29 Page 5 Ln 26

1 Change "W" to m. Add appropriate subscripts to Rho. Change parameters "BD",
2 "PORO", and "VWC" as suggested above. Add in the suggested equation.

3 [Response: Thank you for these suggestions. We changed these symbols as suggested.](#)

4

5 Page 7 Ln 24

6 Again, you need some text about your assumptions regarding water content, phase
7 state, and T_f . Do you assume that water content changes according to characteristic
8 freezing curve, or does all water turn to ice at $T < T_f$? What is T_f ? Is it a particular
9 temperature, is it at a depressed freezing point or is it 0, or does T_f change
10 according to a freezing curve. Just tell the reader what you assume.

11 [Response: Thank you for this comment. We added the following sentence at end of Section](#)
12 [2.3.1.](#)

13 “ T is temperature of soil ($^{\circ}\text{C}$) and T_f is a constant freezing point temperature of soil (0°C). In
14 DOS-TEM, freezing or thawing processes are assumed to happen at T_f , which is consistent
15 with what happens in most land surface models (e.g. Oleson et al. 2010).”

16

17 Page 10 Ln 20

18 You can use symbols here for these defined terms

19 [Response: Thank you for this suggestion. We used symbols as suggested.](#)

20

21 Page 11 Ln 7

22 Saturation? See comments on Figure 4. Check the rest of the text if you really mean
23 to say saturation instead of wetness.

24 [Response: Thank you for this suggestion. We used soil saturation throughout the text and](#)
25 [figures.](#)

26

27 Page 11 Ln 10

1 Anywhere you are referring to a term already defined by a symbol, you can use the
2 symbols to shorten the word count and increase clarity. You can sift through the
3 whole paper this way.

4 Response: Thank you for this suggestion. We used symbols as suggested throughout the
5 whole paper.

6

7 Page 13 Ln 3

8 Mention differences when porosity determined from bulk density is used as shown in
9 Figure S8a and S8b.

10 Response: Thank you for this suggestion. We added the following sentences in Section 3.2.3:

11 When ϕ_m was replaced with ϕ_c , the mean RMSEs and standard deviations were about 0.55
12 m and 0.12 m, respectively.

13

14 And in Section 3.2.4:

15 When ϕ_m was replaced with ϕ_c , the mean RMSEs and standard deviations were about 4.78
16 m and 2.82 m, respectively.

17

18 Page 18 Ln 1

19 I am not sure what standard method you are referring to. The reviewer was simply
20 asking about the common practice of using a vacuum to establish saturation so that
21 no air is left in the sample. The reviewer's question was about properly saturating
22 samples before determining porosity. Drying a soil is sufficient to reach the dry soil
23 state.

24 Response: Sorry for our misunderstanding of the meaning of the reviewer. We rewrote this
25 text in Section 4.3.1:

26

27 There is a variety of methods for measuring soil porosity (Stephens et al., 1998). The method
28 used in this study is widely used for its simplicity (e.g. Chen et al., 2012), and only requires

1 measuring weights of samples under saturation and dry conditions (Equation 2). Soil samples
2 were immersed in water for 24 h to research saturation. It is possible that some air still
3 remained in soil after 24 h immersion under atmospheric pressure, although most of our soil
4 samples contained coarse fragments. It is ideal to immerse soil samples in water under a
5 vacuum condition to draw air out of soil samples completely in future studies.

6 Reference:

7 Stephens, D. B., K. Hsu, M. A. Prieksat, M. D. Ankeny, N. Blandford, T. L. Roth, J. A.
8 Kelsey, and J. R. Whitworth: A comparison of estimated and calculated effective porosity,
9 *Hydrol. Process*, 6, 156-165, 1998

10 Page 18 Ln 9

11 You will want to re-write this in terms of establishing saturated soil conditions

12 Response: Thank you for this suggestion. We rewrote the following sentences:

13

14 "It is possible that some air still remained in soil after 24 h immersion under atmospheric
15 pressure, although most of our soil samples contained coarse fragments. It is ideal to immerse
16 soil samples in water under a vacuum condition to draw air out of soil samples completely in
17 future studies."

18

19

20 Page 20 Ln 1

21 You should quantify these statements to add some interest for the reader who is
22 looking for highlights to cite.

23 Response: Thank you for this suggestion. We quantified the reduction of model errors for
24 both active layer depth and permafrost low boundary. There are several layers for both soil
25 temperature and moisture, and it is difficult to briefly quantify them in the conclusion.
26 Therefore, we did not quantify statements in the conclusion about soil temperature and
27 moisture.

28

1 “When default sand or loam parameters were substituted with measured soil properties, the
2 model errors of active layer depth were reduced by 74% or 84%, respectively. Those of
3 permafrost low boundary were reduced 35% or 34%, respectively.”

4

5

6 Table 1

7 After term, indicate symbol used in brackets. Then, use the symbols in the table
8 headings.

9 [Response: Thank you for this suggestion. We added symbols as suggested.](#)

10

11 Figure 4 and 5

12 Labels in legends should be capitalized as with your other figures to be consistent.
13 “loam” becomes “Loam”, etc.

14 [Response: Thank you for this suggestion. We modified the figure as suggested.](#)

15

16

17

1 **The physical properties of coarse fragment soils and their**
2 **effects on permafrost dynamics: A case study on the**
3 **central Qinghai-Tibetan Plateau**

4 **Shuhua Yi^{1,2}, Yujie He^{3*}, Xinlei Guo⁴, Jianjun Chen^{5,6}, Qingbai Wu⁷, Yu Qin²,**
5 **and Yongjian Ding^{2,8,9}**

6 ¹. School of Geographic Sciences, Nantong University, 999 Tongjing Road, Nantong, 226007,
7 China

8 ². State Key Laboratory of Cryospheric Sciences, Northwest Institute of Eco-Environment and
9 Resources, Chinese Academy of Sciences, 320 Donggang West Road, 730000, Lanzhou,
10 Gansu, China

11 ³. Chinese Research Academy of Environmental Sciences, No.8 Dayangfang, Chaoyang
12 District, 100012, Beijing, China

13 ⁴. Department of Ecosystem and Landscape Dynamics, Institute for Biodiversity and
14 Ecosystem Dynamics, University of Amsterdam, Science Park 904, 1098 XH Amsterdam,
15 The Netherlands

16 ⁵. College of Geomatics and Geoinformation, Guilin University of Technology, 12 Jiangan
17 Road, Guilin, 541004, China

18 ⁶. Guangxi Key Laboratory of Spatial Information and Geomatics, 12 Jiangan Road, Guilin,
19 541004, China

20 ⁷. State Key Laboratory of Frozen Soil Engineering, Northwest Institute of Eco-Environment
21 and Resources, Chinese Academy of Sciences, 320 Donggang West Road, 730000,
22 Lanzhou, Gansu, China

23 ⁸. Key Laboratory of Ecohydrology of Inland River Basin, Chinese Academy of Sciences,
24 Lanzhou 730000, China

25 ⁹. University of Chinese Academy Sciences, Beijing, 100049, China

26 *Co-first Author

27 *Correspondence to:* Yongjian Ding (dyj@lzb.ac.cn)

28 **Abstract.** Soils on the Qinghai-Tibetan Plateau (QTP) have distinct physical properties from
29 agricultural soils due to weak weathering and strong erosion. These properties might affect
30 permafrost dynamics. However, few studies have investigated both quantitatively. In this
31 study, we selected a permafrost site on the central region of the QTP and excavated soil
32 samples down, to 200 cm. We measured soil porosity, thermal conductivity, saturated
33 hydraulic conductivity and matric potential in the laboratory. Finally, we ran a simulation
34 model replacing default sand or loam parameters with different combinations of these
35 measured parameters. Our results from the soil profile showed that coarse fragment soils
36 (diameter >2 mm) ~~was~~ were ~55% on average ~~in soil profile~~, soil porosity was less than 0.3
37 m³ m⁻³, saturated hydraulic conductivity ranged from 0.004-0.03 mm s⁻¹, ~~and~~ and saturated

1 matric potential ranged from -14 to -604 mm. When default sand or loam parameters were
2 substituted with these measured values, the model errors of soil temperature, soil liquid water
3 content, active layer depth and permafrost lower boundary were reduced. The root mean
4 squared errors of active layer depths simulated using measured parameters versus the default
5 sand and loam parameters were about 0.28, 1.06, 1.83 m, respectively. Among these
6 measured parameters, porosities ~~, which were much smaller than for soil textures used in land~~
7 ~~surface models,~~ played a dominant role in reducing model errors and were much smaller than
8 for soil textures used in land surface models. We also demonstrated that soil water dynamic
9 processes should be considered, rather than using static properties under frozen and unfrozen
10 soil states as in most permafrost models. We conclude that it is necessary to consider the
11 distinct physical properties of the coarse fragment soils and water dynamics on the QTP when
12 simulating dynamics of permafrost. ~~It-Thus it~~ is important to develop methods for systematic
13 ~~measuring-measurement of~~ physical properties of coarse fragment soils and to develop a
14 related spatial dataset for porosity ~~because of its importance in simulating permafrost~~
15 ~~dynamics in this region~~.

16 **Key words:** Terrestrial Ecosystem Model; Active layer; Sensitivity test; Soil temperature;
17 Soil water content; Porosity; Coarse fragment soils

18 1 Introduction

19 Permafrost ~~eovers-underlies~~ 25% of Earth's surface. Degradation of permafrost has been
20 reported extensively in Alaska, Siberia and the Qinghai-Tibetan Plateau (QTP; Boike et al.,
21 2013; Jorgenson et al., 2006; Wu and Zhang, 2010). Permafrost thaw has global impacts by
22 releasing large quantities of soil carbon previously preserved in a frozen state and enhancing
23 concentrations of atmospheric greenhouse gases, which will promote further atmospheric
24 warming and degradation of permafrost (Anisimov, 2007; McGuire et al., 2009). Permafrost
25 dynamics also have local to regional impacts on ecosystems by altering soil thermal and
26 hydrological regimes (Salmon et al., 2015; Wang et al., 2008; Wright et al., 2009; Ye et al.,
27 2009; Yi et al., 2014a). In addition, degradation of permafrost affects infrastructure, such as
28 QTP railways and roads (Wu et al., 2004) or the Trans-Alaska Pipeline System in Alaska
29 (Nelson et al., 2001). Therefore, it is critical to develop mitigation and adaptation strategies in
30 permafrost regions for ongoing climate change. Accurate projection of the degree of
31 permafrost degradation is a prerequisite for developing these strategies.

1 Significant effort has been made to improve modeling accuracy and efficiency of
2 permafrost dynamics along two primary lines of inquiry. One is to create suitable freezing and
3 thawing algorithms for different applications, including land surface models (Chen et al.,
4 2015; Oleson et al., 2010; Wang et al., 2017), permafrost models (Goodrich, 1978; Langer et
5 al., 2013; Qin et al., 2017), and other related models (Fox, 1992; Woo et al., 2004). The other
6 line of inquiry is focused on schemes of soil physical properties (Chen et al., 2012; Zhang et
7 al., 2011), which play a critical role in permafrost dynamics. For example, porosity
8 determines the maximum amount of water that can be contained in a soil layer, thermal
9 properties determine the heat conduction within soil layers, and hydraulic properties
10 determine the exchange of soil water between soil layers. The soil water content also
11 determines the large amount of latent heat lost or gained by freezing or thawing, respectively.
12 On the QTP, soil is coarse due to weak weathering and strong erosion (Arocena et al., 2012).
13 Soils with gravel content (particle diameter >2 mm) have been reported in several studies
14 (Wang et al., 2011; Wu et al., 2016; Yang et al., 2009; Qin et al., 2015; Chen et al., 2017; Du
15 et al., 2017). These gravelly soil properties are likely different from those used in current
16 modeling studies (Wang et al., 2013). For example, soil properties in Community Land Model
17 are calculated from fractions of sand, silt and clay based on measurements of agriculture soils
18 (Oleson et al., 2010). However, ~~soil~~the physical properties of coarse fragment soils on the
19 QTP and their effects on permafrost dynamics are under studied (Pan et al., 2017).

20 In this case study we investigated the characteristics of soil physical properties at a site on
21 the central QTP and their effects on permafrost dynamics. We first measured soil physical
22 properties of excavated soil samples in a laboratory. We then conducted a sensitivity analysis
23 with an ecosystem model by substituting the default soil physical properties with those that
24 we measured. We aimed to emphasize the effects of coarse fragment content on soil physical
25 properties and on permafrost dynamics, rather than develop general schemes of soil physical
26 properties for using in modeling studies on the QTP.

27 **2 Methods**

28 **2.1 Site description**

29 The site (34°49'46.2" N, 92°55'56.58" E, 4,628ma.s.l.) is located in the Beiluhe basin, in the
30 continuous permafrost region of the central QTP (Figure 1a, Zou et al. 2017). Based on the
31 map of Li et al. (2015), soils of this region belong to Gelisols and Inceptisols, which occupy
32 34% and 28% of the total area of permafrost region of the QTP, respectively. Land surface

1 types include alpine meadow, alpine steppe, barren surface and thermokarst lakes (Figure 1b;
2 Lin et al., 2011).

3 The site is on top of upland plain landforms, which are formed from fluvial and deluvial
4 sediments. The surficial sediments are dominated by fine to gravelly sands and stones (Figure
5 2; Yin et al., 2017). Soils ~~of at~~ this site ~~belongs to~~ are Inceptisols (Dr. ~~Li~~, Wangping ~~Li~~, ~~of~~
6 Lanzhou University of Technology, personal communication) that are commonly underlain
7 by mudstone. Mudstone is common beneath soil. The plant community type is mainly alpine
8 meadow which is dominated by monocotyledonous species, primarily Poaceae and
9 Cyperaceae. The dominant species are *Kobresia pygmaea*, accompanied *Elymus nutans*,
10 *Carex moorcroftii*, *Oxytropis pusilla*, *Tibetia himalaica*, *Leontopodium nanum* ~~—~~ and
11 *Androsace tapete* (Figure 2c-e).

带格式的: 字体: 非倾斜

12 A weather station was set up in 2002 (Figure 2a) to measure air temperature and relative
13 humidity (2.2m, HMP45C-L11 /L36, Campbell Scientific Inc.), solar radiation (MS-102,
14 EKO, Japan) ~~—~~ and precipitation (QMR102, Vaisala Company). Soil temperatures were
15 measured at depths of 5, 10, 20, 40, 80 ~~—~~ and 160 cm using a PT-100 (EKO, Japan); soil
16 moistures were measured at depths of 20, 40, 80 ~~—~~ and 160 cm using a CS616-L50 (EKO,
17 Japan). A CR3000 data logger (Campbell Scientific Inc., USA) was used to store these data at
18 30 minute intervals. These readings were averaged or summed (e.g. precipitation) into
19 monthly values to drive and validate the model. Based on measurements, multi-year mean
20 annual air temperature, precipitation, downward solar radiation and relative humidity were -
21 3.61 °C, 365.7 mm, 206.3 W m⁻² and 51.1%, respectively (Figure 3). The multi-year mean
22 summer (June to August) air temperature and precipitation were 5.27 °C and 248.3 mm,
23 respectively. The multi-year mean winter (December to February) air temperature and
24 precipitation were -12.44 °C and 5.3 mm, respectively. The multi-year mean annual, summer,
25 and winter soil temperatures at 40 cm were 0.17, 6.65 ~~—~~ and -7.15 °C, respectively. Those at
26 80 cm were 0.11, 4.32 ~~—~~ and -4.86 °C, respectively

27 A borehole was drilled in 2002, and thermistors made by the State Key Laboratory of
28 Frozen Soil Engineering, Chinese Academy of Sciences were installed at 0.5 m intervals from
29 0.5 to 10 m, at 2 m intervals from 12 to 30 m, at 4 m intervals from 34 to 50 m., and at 55 and
30 60 m. Temperature accuracy of this type of thermistor is ±0.05 °C (Wu et al., 2016). The
31 temperatures were recorded on the 5th and 20th days of each month using CR3000 data
32 logger (Campbell Scientific Inc., USA). Based on the our measurements, active layer depth is
33 ~3.3 m, depth of zero annual amplitude is ~6.2 m, and the lower boundary of permafrost is at

1 a depth of ~20 m. The multi-year mean ground temperatures at 0.5, 6, and 60 m are about -
 2 | 0.52, -0.30, and 1.81 °C, respectively.
 3

4 2.2 Soil sampling and measurement

5 Permafrost dynamics are affected by atmosphere, vegetation, and soil textures, therefore, we
 6 excavated soil close to the weather station and borehole (Figure 2a) down to 2 m (Figure 2b) in
 7 August 2014. We used cut rings (10 cm diameter, 6.37 cm height and 500 cm³) to take soil
 8 samples at depth ranges of 0-10, 10-20, 20-30, 40-50, 70-80, 110-120, 150-160, and 190-200
 9 cm. Three replicates were sampled from the top of each depth range and sealed for analysis in
 10 the laboratory. Above 120 cm in the soil pit, coarse soil material was small enough in the cut
 11 rings. Below 150 cm, the material is weathered mudstone, which could also be sampled with
 12 our cut rings. Based on the excavated soil pit and measured soil temperature, this site belongs to
 13 Inceptisols with suborder of Gelept (soil taxonomy, ST, Soil Survey Staff, 2014). The soil pit
 14 consists of A horizon (~20 cm), Bw horizon (~20-80 cm) and C material dominated by
 15 fractured bedrock.

16 We used the KD2 Pro (Decagon, US) to measure thermal conductivity of soil samples. The
 17 steps we took to determine soil properties for each sample were as follows: 1) the soil sample
 18 | was dried in an oven and weighed (0.001g precision) to calculate bulk density; Then-then 2) the
 19 soil sample was exposed to a constant temperature (20°C) for 24 h, a certain volume of water
 20 was injected into the soil samples, and KD2 Pro (Decagon, USA) was used to measure the
 21 thermal conductivity; Next-next 3) the sample and the KD2 probe were put into a refrigerator
 22 | at -15°C for 12 h and thermal conductivity was measured again; 4) Steps-steps 2 and 3 were
 23 repeated at increasing levels of soil volumetric water content until soil samples were up to the
 24 | point of saturation; Finally-finally 5), the soil sample was immersed in water for 24 h and
 25 weighed to calculate porosity, and the saturated unfrozen and frozen thermal conductivity were
 26 | then measured, accordingly. The bulk density (ρ_b , g cm⁻³), porosity (ϕ_m , m³ m⁻³)
 27 and volumetric water content (θ_{liq} , m³ m⁻³) were calculated with the following
 28 equations.

$$29 \quad \rho_b = \frac{W_{dry} - W_{cr}}{V_{cr}} \quad (1)$$

$$30 \quad \phi_m = \frac{W_{sat} - W_{dry}}{V_{cr} \rho_w} \quad (2)$$

带格式的：下标

带格式的：上标

带格式的：下标

带格式的：上标

带格式的：上标

带格式的：下标

带格式的：德语(德国)

$$\theta_{liq} = \frac{W_{all} - W_{dry}}{V_{cr}} / \rho_w \quad (3)$$

Where W_{dry} , W_{sat} , W_{all} , W_{cr} are mass of oven dried sample, saturated sample, sample with some water with cut ring, and empty cut ring (g), respectively. V_{cr} is the volume of cut ring (cm^3). ρ_w is the density of water (1 g cm^{-3}). We also calculated porosity from bulk density ($\phi_c, \text{g m}^{-3}$):

$$\phi_c = 1 - \frac{\rho_b}{\rho_p} \quad (4)$$

Where ρ_p is particle density (2.65 g cm^{-3}).

- 带格式的: 下标
- 带格式的: 非上标/ 下标
- 带格式的: 德语(德国)

We used pressure membrane instruments (1500F1, Soilmoisture Equipment Corp, US) to measure the matric potential of soil samples (Azam et al., 2014; Wang et al., 2007), using both 15 bar and 5 bar pressure chambers. Pressure values were set at 0, 10, 20, 40, 60, 80, 100, 150, 200, 300, and 400 kpa. It usually took 3-4 days to finish one measurement at one pressure level. We used a soil permeability meter (TST-70, Nanjing T-Bota Sciotech Instruments & Equipment Co., Ltd. China) to measure saturated hydraulic conductivity of soil samples (Gwenzi et al., 2011). Finally, soil samples were sieved through a 2.0 mm mesh, and soil particle size distribution was determined with a laser diffraction analyzer (Malvern-2000, Worcestershire, UK).

2.3 Model description

To simulate soil temperatures, soil liquid water content, temperature in rock layers, active layer depth (ALD) and permafrost low boundary (PLB) dynamics we used The model used in this study is a dynamic organic soil version of Terrestrial Ecosystem Model (DOS-TEM). Models from the TEM family simulate the carbon and nitrogen pools of vegetation and soil, and their fluxes among atmosphere, vegetation, and soil (McGuire et al., 1992). They have been widely used in studies of cold region ecosystems (e.g. McGuire et al., 2000; Yuan et al., 2012; Zhuang et al., 2004; 2010). The DOS-TEM consists of four modules, environmental, ecological, fire disturbance, and dynamic organic soil (Yi et al., 2010). The environmental module operates on a daily time interval using mean daily air temperature, surface solar radiation, precipitation, and vapor pressure, which are downscaled from monthly input data (Yi et al., 2009b). The module takes into account radiation and water fluxes among the atmosphere, canopy, snow pack, and soil. Soil temperatures, soil liquid water content,

~~temperature in rock layers, active layer depth (ALD) and permafrost low boundary (PLB) were simulated explicitly.~~

2.3.1 Implementation of soil thermal processes

Earlier versions of TEM did not simulate soil temperature (McGuire et al., 1992). Zhuang et al. (2001) incorporated Goodrich (1978) permafrost model into TEM. Yi et al. (2009a) incorporated a two-directional Stefan algorithm to simulate soil freezing and thawing for complex soils with changes in soil organic and moisture content. Temperatures of all soil layers in the DOS-TEM are updated daily. Phase change is calculated first before heat conduction. A two-directional Stefan algorithm is used to predict the depths of freezing or thawing fronts within the soil (Woo et al., 2004). It first simulates the depth of the front in the soil column from the top downward, using soil surface temperature as the driving temperature. It then simulates the front from the bottom upward using the soil temperature at a specified depth beneath a front as the driving temperature (bottom-up forcing). The latent heat used for phase change is recorded for each soil layer. If a layer contains n freezing or thawing fronts, this layer is then explicitly divided into $n+1$ soil layers. All soil layers are grouped into 3 parts: 1) those above the uppermost freezing or thawing front; 2) those below the lowermost freezing or thawing front; and 3) those between the uppermost and lowermost fronts. Soil temperatures are then updated by solving finite difference equations of each part with latent heat from phase change as an energy source or sink (Yi et al., 2014a). Soil surface temperature, which is used as a boundary condition, is calculated using daily air maximum, air minimum, radiation, and leaf area index (Yi et al., 2013).

The version of the DOS-TEM in this study uses the Côté and Konrad (2005) scheme to calculate thermal conductivity (Yi et al., 2013; Pan et al., 2017), which is also been used by other studies on the QTP (e.g. Chen et al., 2012, Luo et al., 2009), and is as follows:

$$\lambda = \begin{cases} k_e \lambda_{sat} + (1 - k_e) \lambda_{dry} & s > 10^{-5} \\ \lambda_{dry} & s \leq 10^{-5} \end{cases}$$

(45)

where λ , λ_{sat} , λ_{dry} are soil thermal conductivity, saturated soil thermal conductivity, and dry soil thermal conductivity ($\text{W m}^{-1} \text{K}^{-1}$), respectively, and k_e is the Kersten number (Côté and Konrad, 2005). Dry thermal conductivity varies with soil properties according to:

$$\lambda_{dry} = \chi 10^{-\eta\phi}$$

(56)

where χ ($\text{W m}^{-1} \text{K}^{-1}$) and η (no unit) are parameters accounting for particle shape effects, which are specified for gravel, fine mineral and organic soil (Côté and Konrad, 2005), and ϕ is porosity. Saturated thermal conductivity varies with water content and phase state according to:

$$\lambda_{sat} = \begin{cases} \lambda_s^{1-\phi} \lambda_{liq}^\phi & T \leq T_f \\ \lambda_s^{1-\phi} \lambda_{ice}^\phi & T > T_f \end{cases}$$

(67)

where λ_{liq} , λ_{ice} , λ_s are thermal conductivities of liquid water, ice, and soil solid ($\text{W m}^{-1} \text{K}^{-1}$), which are all constant values. T is temperature of soil ($^\circ\text{C}$) and T_f is a constant freezing point temperature of soil (0°C). In DOS-TEM, freezing or thawing processes are assumed to happen at T_f , which is consistent with what happens in most land surface models (e.g. Oleson et al. 2010). T and T_f are temperature of soil and freezing point temperature of soil ($^\circ\text{C}$), respectively. In DOS-TEM, freezing or thawing processes are assumed to be happened at T_f , following most of the land surface models (e.g. Oleson et al. 2010).

带格式的: 字体颜色: 自动设置

带格式的: 字体颜色: 自动设置

带格式的: 字体颜色: 自动设置

2.3.2 Implementation of soil hydrological processes

Surface runoff, infiltration, and water redistribution among soil layers are simulated in a similar way as Community Land Model 4 (Oleson et al., 2010). Soil matric potential (Ψ) determines the direction of water movement, and hydraulic conductivity describes the ease with which water can move through the soil.

$$\Psi = \Psi_{sat} \left(\frac{\theta_{liq}}{\phi} \right)^{-B}$$

(78)

where Ψ_{sat} is saturated soil matric potential ($\text{mm H}_2\text{O}$, hereafter mm), θ_{liq} is volumetric liquid water content ($\text{m}^3 \text{m}^{-3}$), and B is pore size distribution parameter. The soil hydraulic conductivity (K , mm s^{-1}) is a function of the saturated soil hydraulic conductivity (K_{sat}) as follows:

$$K = K_{sat} \left(\frac{\theta_{liq}}{\phi} \right)^{2B+3}$$

(89)

1 Several important features relating to permafrost have been considered in the DOS-TEM
2 (see Yi et al., 2014b), including runoff from a perched saturated zone or exchanges of water
3 between the soil and a water reservoir. Runoff from a perched saturated zone above
4 permafrost is implemented following Swenson et al. (2013):

$$5 \quad Q_{perch} = \alpha k_p (z_{frost} - z_{perched}) \sin\left(\frac{\theta}{180} \pi\right)$$

6 | (910)

7 where α is an adjustable parameter (0.6 m^{-1}), K_p is the mean saturated hydraulic conductivity
8 within the perched saturated zone (mm s^{-1}), z_{frost} and $z_{perched}$ are the depths to the permafrost
9 | table and the perched water table (m), respectively, and θ is slope ($^\circ$).

10 The DOS-TEM has been verified against the Neumann Equation for water, mineral and
11 organic soil under an idealized condition (Yi et al., 2014b), and validated against field
12 measurements for various locations in Alaska, the Arctic, and the QTP (Yi et al., 2009b, Yi et
13 al., 2013, Yi et al., 2014a).

14 **2.4 Model inputs and initialization**

15 We used the monthly averaged air temperature, downward radiation, precipitation and
16 humidity as input to drive the DOS-TEM. Leaf area index (LAI), leaf area per unit ground
17 surface area, was specified to be $0.6 \text{ m}^2 \text{ m}^{-2}$ in July and August, $0.1 \text{ m}^2 \text{ m}^{-2}$ in April and
18 | October, $0 \text{ m}^2 \text{ m}^{-2}$ between November and March, and interpolated linearly in other months. It
19 is used in the DOS-TEM to calculate ground surface temperature in combination with other
20 meteorological variables (Yi et al., 2013). Its value is unchanged within each month.

21 Soil temperature and moisture were initialized at $-1 \text{ }^\circ\text{C}$ and saturation. The temperature
22 gradient at the bottom of bedrock was set to be $0.06 \text{ }^\circ\text{C cm}^{-1}$ based on borehole observations.
23 Volumetric unfrozen liquid water in winter was set to be 0.1 based on observations. Multi-
24 year (2003-2012) mean monthly driving data were used to spin up the model for 100 yr. In
25 this way, suitable initial values of soil moisture, temperature and rock temperature of each
26 layer are generated before driving DOS-TEM with monthly data over the period of 2003-2012.

1 2.5 Sensitivity analyses

2 The soil textures on the QTP mainly consist of loam, sand, and coarse fragment soils (Wu and
3 Nan, 2016). We used a uniform sand or loam soil profile to represent coarse and fine soil
4 textures, respectively. Sands are the ~~most coarsest~~coarsest texture considered in most the
5 modeling studies (e.g. Oleson et al., 2010). Therefore, we used our measured parameters to
6 substitute the parameters of sand and loam to investigate the effects of coarse-fragment soil
7 parameters on permafrost dynamics. We first ran DOS-TEM using the default porosity, soil
8 thermal conductivity (Equation 45), hydraulic conductivity (Equation 89), and matric
9 potential schemes of these two default soil textures (Equation 78). The default parameters ϕ
10 Ψ_{sat} , K_{sat} and B were calculated based on soil texture used in Community Land Model
11 (Equations 7-8 and 89; Oleson et al., 2010). We then substituted the default values of ϕ
12 Ψ_{sat} , K_{sat} and B based on our laboratory measurements and calibration. Parameters Ψ_{sat} and
13 B were fitted with measured matric potential data using Isqcurvefit tools of Matlab. We did
14 not calibrate soil thermal conductivity to retrieve parameters of Equations 5-6 and 67. Instead,
15 we interpolated measured thermal conductivities over a range of degrees of saturation (0 to 1),
16 which was used as a lookup table by the DOS-TEM. Therefore, our sensitivity analyses
17 considered a set of 4 factors, i.e. porosity, matric potential (Ψ_{sat} and B), hydraulic conductivity
18 (K_{sat} and B) and thermal conductivity. We also analyzed 3 different slopes (0, 5 $^{\circ}$ and 10 $^{\circ}$)
19 and 3 different soil thicknesses (3.25, 4.25 $_{-2}$ and 5.25 m) above 56 m of bed rock. There were
20 11 soil layers with the top 9 layers being 0.05, 0.1, 0.1, 0.2, 0.2, 0.2, 0.3, 0.3 $_{-2}$ and 0.3 m thick.
21 The thicknesses of the bottom 2 soil layers were 0.5 and 1 m, 0.5 and 2 m, and 1.5 $_{-2}$ and 2 m
22 for the 3.25, 4.25 $_{-2}$ and 5.25 m cases, respectively. There were 6 rock layers with thicknesses
23 of 2, 2, 4, 8, 16 $_{-2}$ and 20 m. Since the site is on the top of upland plain landforms, we did not
24 further test the effects of aspect on radiation on ground surface. We instead considered the
25 effects of slope on surface runoff. In summary, our sensitivity analyses with the DOS-TEM
26 involved 288 different combinations of parameter values.

27 We did not measure the heat capacity. The maximum and minimum heat capacities of mineral
28 soil types considered in land surface model are 2.355 and 2.136 MJ m $^{-3}$, respectively, giving a
29 relative difference less than 10%. Therefore, in this study, we did not make sensitivity tests
30 using thermal diffusivity (the ratio between thermal conductivity and heat capacity).

1 3 Results

2 3.1 Soil physical properties

3 3.1.1 Soil porosity, particle size and bulk density

4 Results from laboratory analysis of the soil samples are shown in Table 1 and 2. The mean
5 ~~weight-mass ratio~~ of the coarse soil fraction (particle size diameter > 2 mm) of different soil
6 layers ranged from 0.38 to 0.65 with a mean of 0.55. According to the USDA classification
7 system (clay (<2 μ m), silt (2 –50 μ m, in this study 2-63 μ m) and sand (50 μ m -2.0 mm,
8 in this study 63 μ m -2.0 mm)), the major soil texture of this site was loamy sand, with the
9 exception of sandy loam at ~~depth of~~ 20-30 cm ~~depth~~. The default porosities of sand and loam
10 were 37.3% and 43.5%, respectively. The ~~φ_m measured porosity~~ of samples down to 2 m
11 depth ranged from 21% to 30% with a mean of 27%, and the mean ~~bulk density- ρ_b~~ ranged
12 from 1.61 to 1.86 g cm⁻³ with a mean of 1.74 g cm⁻³. ~~The φ_c (Equation 4)The porosity~~
13 ~~calculated from bulk density (= 1 - bulk density/2.65 g cm⁻³)~~ ranged from 29.8% to 39.2%. No
14 significant relationships were found among ~~φ_m soil porosity~~, ~~ρ_b bulk density~~, and the coarse
15 soil fraction (p>0.05).

带格式的: 下标

带格式的: 下标

带格式的: 非上标/ 下标

16 3.1.2 Thermal conductivity

17 The results of the thermal conductivity determinations are shown in Table 3. The unfrozen
18 ~~dry soil thermal conductivity λ_{dry}~~ of different soil layers ranged from 0.24 to 0.40 W m⁻¹ K⁻¹
19 with a mean of 0.36 W m⁻¹ K⁻¹, and the frozen ~~λ_{dry} dry soil thermal conductivity~~ ranged from
20 0.25 to 0.41 W m⁻¹ K⁻¹ with a mean of 0.35 W m⁻¹ K⁻¹. The difference of ~~λ_{dry} dry thermal~~
21 ~~conductivity~~ between frozen and unfrozen states was small. The unfrozen ~~saturated soil~~
22 ~~thermal conductivity λ_{sat}~~ of different soil layers ranged from 2.15 to 2.74 W m⁻¹ K⁻¹ with a
23 mean of 2.48 W m⁻¹ K⁻¹. The frozen ~~λ_{sat} saturated soil thermal conductivity~~ ranged from 3.06
24 to 3.72 W m⁻¹ K⁻¹ with a mean of 3.33 W m⁻¹ K⁻¹. The difference of ~~λ_{sat} saturated thermal~~
25 ~~conductivity~~ between frozen and unfrozen states was about 0.85 W m⁻¹ K⁻¹. There existed a
26 threshold of soil ~~wetness saturation~~ (i.e. ~0.28 m³ m⁻³), below which frozen soil thermal
27 conductivity was slightly smaller than unfrozen soil (Figure 4a).

带格式的: 下标

1 Results from determining thermal conductivities using the Côté and Konrad (2005) scheme
2 are shown in Figure 4b. The default ~~dry~~-frozen and unfrozen ~~λ_{dry}~~ thermal conductivities for
3 sand and loam were about 0.42 and 0.24 W m⁻¹ K⁻¹, respectively. The ~~saturated~~-frozen and
4 unfrozen ~~λ_{sat}~~ thermal conductivities of sand were 3.11 and 1.90 W m⁻¹ K⁻¹, respectively. Those
5 of loam were about 2.36 and 1.33 W m⁻¹ K⁻¹, respectively. Results from determining thermal
6 conductivities using the Farouki (1986) scheme are shown in Figure 4c. The default ~~dry~~
7 frozen and unfrozen ~~λ_{dry}~~ thermal conductivities for sand and loam were about 0.97 and 0.63 W
8 m⁻¹ K⁻¹, respectively. The ~~saturated~~-frozen and unfrozen ~~λ_{sat}~~ thermal conductivities of sand
9 were 5.21 and 3.18 W m⁻¹ K⁻¹, respectively. Those of loam were about 4.49 and 2.52 W m⁻¹
10 K⁻¹, respectively.

11 3.1.3 Saturated hydraulic conductivity

12 The mean ~~saturated hydraulic conductivity~~ K_{sat} of soil layers, shown in Table 4, ranged from
13 0.0036 to 0.0315 mm s⁻¹. The maximum ~~saturated hydraulic conductivity~~ K_{sat} was about 8.7
14 times larger than the minimum. The ~~K_{sat}~~ ~~saturated hydraulic conductivity~~ tended to be larger
15 with increasing proportion of coarse fragment in the soil samples (Figure 5a), and was about
16 0.03-0.06 mm s⁻¹ for some samples with coarse fragment greater than 70%. The default
17 ~~K_{sat}~~ ~~saturated hydraulic conductivities~~ of sand and loam were 0.024 and 0.0042 mm s⁻¹,
18 respectively.

带格式的：下标

带格式的：下标

19 3.1.4 Matric potential

20 The correlation coefficients between calculated and fitted ~~Ψ~~ matric potential, shown in Table 4,
21 were all greater than 0.96. The mean absolute value of ~~Ψ_{sat}~~ ~~saturated matric potential~~ of soil
22 layers ranged from 14.47 to 603.7 mm, and those of B ranged from 1.89 to 5.22 (Table 4 and
23 Figure 5b). The default absolute value of ~~Ψ_{sat}~~ ~~saturated matric potential~~ of sand and loam were
24 47.29 and 207.34 mm, respectively, and the B values 3.39 and 5.77, respectively.

带格式的：下标

25 3.2 Comparisons between simulations using default vs. measured parameters

26 3.2.1 Soil temperature

27 The mean root mean squared errors (RMSEs) between monthly measured soil temperatures
28 and model runs with measured parameters using different combination of soil thicknesses
29 (3.25, 4.25, and 5.25 m) and slopes (0, 5, and 10°) were about 1.07 °C at 20 cm (Figure 6c).

1 The mean RMSEs for all model runs with default sand and loam parameters were about 0.97
2 and 1.18 °C, respectively. For other soil layers, the RMSEs of model runs with measured
3 parameters were much smaller than those with default sand and loam parameters (Figures 6d-
4 l). The simulated soil temperatures using default sand and loam parameters were all lower
5 than measured ones in summer at 100 and 200 cm, and in winter at 400 cm. The RMSEs can
6 be as large as 2.53 °C (Figure 6e).

7 The standard deviations of soil temperatures among different slopes and soil thicknesses
8 using measured parameters were larger than those using the default parameters (Figure 6); and
9 they increased from 0.40 °C at 100 cm to 0.61 °C at 200 cm (Figure 6f and i). The standard
10 deviations using default loam parameters were smaller (<0.15 °C at all depths) than those
11 using default sand parameters.

12 3.2.2 Soil liquid water

13 The mean RMSEs between monthly measured θ_{liq} liquid soil volumetric water content
14 (VWC) and model simulations with measured parameters ranged from 0.03 to 0.09, which
15 were smaller than RMSEs for sand and loam parameters (Figure 7). The model simulations
16 for loam parameters have larger RMSEs than those for sand parameters. θ_{liq} VWCs were
17 always overestimated in warm seasons at depths of 10, 40, and 80 cm. θ_{liq} VWCs were
18 underestimated at a depth of 160 cm, where the simulated soil was frozen. All model
19 simulations overestimated θ_{liq} VWC at 40 cm, where the maximum measured θ_{liq} VWCs
20 were about 0.1 (Figure 7d-f).

21 The standard deviations of θ_{liq} VWC among different slopes and soil thicknesses using
22 sand parameters were about 0.077, which were larger than those using measured parameters
23 (~0.062). The standard deviations of θ_{liq} VWC using loam parameters (<0.032) were less
24 than those using measured parameters.

25 3.2.3 Active layer depth (ALD)

26 The mean RMSEs between measured ALDs (derived from linear interpolation of soil
27 temperatures) and modelled ALDs (simulated explicitly) were about 1.06, 1.72, and 0.28 m
28 for model runs with sand, loam, and measured parameters (Figure 8a). The mean standard
29 deviations were about 0.088, 0.026, and 0.28 m. All simulations using sand and loam

带格式的：下标

parameters underestimated ALDs. When ϕ_m was replaced with ϕ_c , the mean RMSEs and standard deviations were about 0.55 m and 0.12 m, respectively.

3.2.4 Permafrost lower boundary (PLB)

The mean RMSEs between measured PLBs (derived from linear interpolation of temperatures) and modelled PLBs (derived from linear interpolation of simulated bed rock temperatures) were about 10.25, 10.23, and 6.71 m for model runs with sand, loam, and measured parameters (Figure 6b8b). The mean standard deviations were about 1.89, 1.51, and 6.62 m. All simulations using sand and loam parameters overestimated PLBs. When ϕ_m was replaced with ϕ_c , the mean RMSEs and standard deviations were about 4.78 m and 2.82 m, respectively.

3.3 Model sensitivity analyses

Deep soil layers used in models are usually specified as being thick. For example, a 1 m thick soil layer was used in our simulations starting around 3 m soil depth. Soil temperatures at this depth are usually close to 0 °C. Therefore, the RMSEs of deep soil layers were small and did not facilitate evaluation of model sensitivities. In the following subsections, we used 20 and 100 cm soil temperatures, ALDs and PLBs for sensitivity analysis.

3.3.1 Effects of single parameter sensitivity analyses

Porosity

Replacing default sand or loam porosity with ~~ϕ_m -measured porosities~~ changed mean RMSEs of soil temperatures (model runs with 3 different slopes and 3 different soil thicknesses at 2 different soil depths) from 1.18 or 1.84 °C to 1.25 or 1.09 °C, respectively (Figure 9 and 10). Mean RMSEs of ALD were reduced from 1.06 or 1.72 m to 0.22 or 0.85 m, respectively. Mean RMSEs of PLB were changed from 10.26 or 10.24 m to 6.61 or 10.97 m. Mean RMSEs of ~~θ_{liq} VWC~~ were reduced from 0.074 or 0.14 to 0.06 or 0.062 when ~~ϕ_m -measured porosities~~ were used for replacing default sand or loam porosity, respectively (Figure 11 and 12).

Thermal conductivity

1 Replacing default sand or loam thermal conductivity with measured thermal conductivity
2 reduced mean RMSEs of soil temperatures from 1.18 or 1.84°C to 1.02 or 1.15°C,
3 respectively (Figure 9 and 10). Mean RMSEs of ALD were reduced from 1.06 or 1.72 m to
4 0.56 or 1.04 m, respectively. Mean RMSEs of PLB were changed from 10.26 or 10.24 m to
5 4.18 or 1.27 m, respectively. Mean RMSEs of θ_{liq} VWC changed very slightly (Figure 11 and
6 12).

7 **Hydraulic conductivity and matric potential**

8 Replacing default sand or loam hydraulic conductivity with measured parameters had very
9 small effects on mean RMSEs of soil temperatures and ALDs (Figure 9 and 10). The same
10 was true for matric potential. When hydraulic conductivity of default sand or loam was
11 substituted, mean RMSEs of PLB decreased or increased, respectively. However, when
12 matric potential was substituted, mean RMSEs of PLBs increased or decreased, respectively.
13 When hydraulic conductivity or matric potential parameters were substituted in default sand
14 or loam parameters, mean RMSEs of θ_{liq} VWC changed slightly (Figure 11 and 12).

15 **3.3.2 Effects of combined parameters**

16 We compared model simulations with different combinations of measured parameters
17 (porosity, thermal conductivity, hydraulic conductivity and matric potential) to those with one
18 substituted measured parameter. We ranked those model runs with less RMSEs than the best
19 of the model runs with one parameter substituted with a measurement-derived value (Table 5
20 and 6). We didn't consider the 10 cm soil temperature, which were similar among all model
21 runs.

22 For sand, model simulations with porosity and thermal conductivity or hydraulic
23 conductivity substituted had 4 outcomes with lower RMSEs (Table 5 and Figures 9 and 11).
24 Only 2 out of 7 outcomes had lower RMSEs with all 4 parameters substituted. Among all the
25 18 cases with RMSEs less than the individual "best" RMSE, porosity was included 18 times,
26 ~~followed by~~ and thermal conductivity and hydraulic conductivity ~~both with~~ were included 10
27 times.

28 For loam, model simulations with porosity and thermal conductivity substituted had 5
29 outcomes with lower RMSEs (Table 6 and Figures 10 and 12). Among all the 27 cases with

1 RMSEs less than the individual “best” RMSE, porosity was included 27 times, followed
2 by and thermal conductivity with was included 16 times, and matric potential with 14 times.

3 3.3.3 Effects of slope and soil thickness

4 Changes of slope alone had small effects on simulated soil temperatures and ALDs (Figures 9
5 and 10). An increase of slope generally reduced RMSEs of θ_{liq} VWCs (Figures 11 and 12).
6 Model simulations with porosity substituted had smaller differences in θ_{liq} VWC RMSE
7 between different cases of slopes. For example, the mean RMSEs of model simulations with
8 slopes of 0° or 5° and sand parameters substituted with ϕ_m measured porosity were 0.078 or
9 0.048, respectively. While those with porosity not substituted were 0.141 or 0.055,
10 respectively. Similarly, the mean RMSEs of model simulations using default loam parameters
11 with porosity substituted were 0.08 or 0.05 for slope of 0° or 5° , respectively. The mean
12 RMSEs were 0.18 or 0.1 with porosity not substituted, respectively. For a further increase of
13 slope to 10° , changes of RMSEs of θ_{liq} VWCs at depths of 10-160 cm were small.

带格式的：下标

14 Soil thickness had small effects on 20 and 100 cm soil temperatures and 10-160 cm θ_{liq}
15 VWCs, and it had prominent effects on PLB for a few cases only with a slope of 10°
16 (Figures 9 and 10).

17 4 Discussion

18 4.1 Characteristics of soil physical properties

19 Although the effects of coarse fragment soils on permafrost dynamics have been considered
20 in a few modelling studies, the thermal and hydraulic properties of coarse fragment soils were
21 calculated without validation or calibration (Pan et al., 2017; Wu et al., 2018). To our
22 knowledge, this is the first study measuring physical properties of coarse fragment soil
23 samples from permafrost region of the QTP.

24 The weight fraction of coarse fragment (diameter > 2mm, including gravel) in the soil
25 samples we analysed was greater than 55% on average. While the typical soil types
26 considered in land surface models and other models usually have much smaller diameter. For
27 comparison, the fractions of gravel considered in Pan et al. (2017) ranges from 5% to 33%
28 and from 10% to 28% for the Madoi and Naqu sites, respectively. The Beiluhe site and the

1 aforementioned sites are located in regions with Gelisols and Inceptisols, which occupy ~62%
2 of the permafrost regions of the QTP (Li et al., 2015). It is possible that coarse fragment soils
3 commonly exist on the QTP. The dataset of Wu and Nan (2016) indicated that gravel content
4 widely exists on the middle and western part of the QTP. The saturated hydraulic conductivity
5 and matric potential of soil samples measured in this study were more similar to sand than to
6 loam (see Section 3.1). It is consistent with the study of Wang et al. (2013) that coarse soil
7 material has poor water holding capability.

8 The measured thermal conductivities of saturated soil samples were relatively close to
9 those estimated by the Côté and Konrad (2005) scheme. But they were much less than those
10 estimated by the Farouki scheme (Figure 4). Several other studies also found that Farouki
11 scheme overestimated soil thermal conductivity (Chen et al. 2012; Luo et al., 2009).

12 One important finding of this study is the relatively small value of porosity. The measured
13 porosity ranged from 0.206 to 0.302, which is less than those of soil types considered in land
14 surface models. For example, the porosities of mineral soil types considered in Community
15 Land Model range from 0.37 to 0.48 (Oleson et al., 2010). Porosity determines the maximum
16 water stored in a soil layer, and affects soil thermal conductivity, hydraulic conductivity and
17 matric potential (Equation 56-89). It plays a more important role than other parameters in
18 simulated soil thermal and hydrological dynamics (Table 5 and 6; Figure 9-12). It is
19 noteworthy that it is easy and efficient to measure porosity.

20 **4.2 Effects of soil water on permafrost dynamics**

21 Soil water not only affects soil thermal properties (e.g. thermal conductivity and heat
22 capacity), but also affects the amount of latent heat lost or gained, for freezing or thawing,
23 respectively (Goodrich, 1978; Farouki, 1986). Soil water is determined by infiltration,
24 evapotranspiration, water movement among soil layers, subsurface runoff and exchange with
25 a water reservoir. Therefore, processes or parameters that affect soil water dynamics will also
26 affect permafrost dynamics. This study quantitatively assessed the effects of soil water on
27 permafrost dynamics. For example, when default loam parameters with high porosity and low
28 saturated hydraulic conductivity were used, soil layers were almost saturated (Figure 7). The
29 simulated ALDs were about 1.58 m, which was less than half of measured ALDs (Figure 8a).
30 When the slope was 0°, subsurface runoff didn't occur in the saturated zone above the bottom
31 of the active layer. The simulated soil water content was generally higher in the active layer.

1 However, when the slope was 5°, the simulated soil water content was less and the RMSE was
2 smaller (Figure 11 and 12). These patterns were especially obvious when both porosity and
3 saturated hydraulic conductivity were large (Equation 910; Figure 11 and 12). Other studies
4 have also emphasized the importance of subsurface runoff above the bottom of the active
5 layer (Frey and McClelland, 2009; Walvoord and Striegl, 2007). The effects of soil water
6 content on soil thermal dynamics increased with soil and rock depth (Figure 9 and 10). The
7 biggest effects were on PLB, which became manifest during long-term spinup procedures.

8 Land surface models generally represent soil water dynamics (e.g. Chen et al., 2015;
9 Oleson et al., 2010; Wang et al., 2017). However, the thermal processes in permafrost models
10 usually use specified thermal properties, which were static during model simulations (Li et al.,
11 2009; Nan et al., 2005; Qin et al., 2017; Zou et al., 2017). As shown in this study, ~~soil thermal
12 and hydrological properties depend largely on~~The variation of soil water content in coarse
13 fragment soils strongly affects thermal and hydrological properties, thus it ~~is~~ is critical to
14 simulate soil water dynamics to properly project permafrost dynamics in the future.

15 4.3 Limitations and Outlook

16 4.3.1 Sampling and laboratory measurement

17 We used cut rings with 10 cm diameter to sample soil and weathered mudstones. However, it
18 is very likely that there could have been much bigger coarse fragment soils. Therefore, larger
19 containers should be used to take samples for further laboratory analysis in the future.

20 During our laboratory work, we found two phenomena. First, we originally used the QL-
21 30 thermophysical instrument (Anter Corporation, US) to measure thermal conductivity. It
22 worked properly under unfrozen condition. However, when frozen, the surface of the soil
23 sample was usually uneven due to frost heave, which reduces the contact between the QL-30
24 plate and the soil sample surface. The measured frozen thermal conductivities were smaller
25 than unfrozen thermal conductivity even for the case of saturation, which were definitely
26 wrong, thus we used the KD2 pro to determine thermal conductivities. The second
27 phenomenon was that there seems to be a threshold of soil ~~wetness~~saturation, below which
28 unfrozen soil thermal conductivity is greater than frozen soil thermal conductivity (Figure 4a).
29 This pattern was somewhat exhibited in estimates of the Côté and Konrad (2005) scheme

(Figure 4b), but not in the estimates of the Farouki scheme (Figure 4c). More measurements using instruments with higher accuracy should be made in the future.

~~It is ideal to draw water in soil samples under a vacuum condition before weighing dry soil sample. Unfortunately, we do not have such instrument. We dried soil samples in an oven at 65 °C for over 48 h, which is commonly used in ecological studies, e.g. Qin et al. (2018). The measured porosities are generally smaller than those calculated from bulk density. We made additional model simulations using porosities calculated from bulk density in combination with other measured parameters. Our R_r results showed that the RMSEs of ALD and PLB were 0.55 m and 4.78 m, respectively (Figures not shown). While, whereas those used measured porosities calculated using $-\phi_m$ were 0.28 m and 6.71 m, respectively. Considering the importance of porosity on simulated permafrost dynamics, it is important to draw water out of soil samples in a vacuum condition before weighing dry soil samples in the future. There is a variety of methods for measuring soil porosity (Stephens et al., 1998). The method used in this study is widely used for its simplicity (e.g. Chen et al., 2012), and only requires measuring weights of samples under saturation and dry conditions (Equation 2). Soil samples were immersed in water for 24 h to research saturation. It is possible that some air still remained in soil after 24 h immersion under atmospheric pressure, although most of our soil samples contained coarse fragments. It is ideal to immerse soil samples in water under a vacuum condition to draw air out of soil samples completely in future studies.~~

4.3.2 Model simulation

Although the DOS-TEM using measured parameters provided satisfactory results, there are some aspects requiring further improvement in the future. For example, the measured soil moistures at 40 cm depth were less than $0.1 \text{ m}^3 \text{ m}^{-3}$. However, the simulated soil moistures were always much greater (Figure 7f). There were also spikes in measured soil moistures at 80 and 160 cm depths, which were not presented in the simulation (Figure 7 i and l). In the DOS-TEM, the unfrozen soil water content, or supercold water, was prescribed to be $0.1 \text{ m}^3 \text{ m}^{-3}$. When soil is freezing, if soil liquid water content is less than this value, no phase change will happen (Figure 7k). Therefore, model results would improve with the capability to simulate the dynamics of unfrozen soil water content (Romanovsky and Osterkamp, 2000).

~~The TEM family models use monthly atmospheric data as driving for both site and regional applications. In this study, 30 min and daily driving data are available. Although it is~~

带格式的: 缩进: 首行缩进: 1 厘米

possible to lose fidelity after daily interpolations, we still decided to use monthly driving data for the following reasons: 1) Zhuang et al. (2001) performed a test with daily and monthly driving datasets. The results showed that the root mean squared errors of active layer depth were about 3 cm; 2) we will apply the model over large regions where reliable daily datasets might not be available.

带格式的: 德语(德国)

4.3.3 Regional applications

Coarse fragment soils affect soil physical properties. For example, soil porosity and saturated hydraulic conductivity are determined by the fraction of gravel, diameter, and degree of mixture (Zhang et al., 2011). ~~Thus Soil-soil~~ texture plays an important role in permafrost dynamics (Figure 8). ~~However, the~~ ~~The~~ dominant soil texture on the QTP from Wu and Nan (2016) are loam, sand, and gravel. The specification of loam in simulations results in estimates of ALD that are much smaller than measurements (Yi et al., 2014a). To properly simulate the distribution and dynamics of permafrost on the QTP under climate change scenarios, it is important to develop proper schemes of soil physical properties in relation to coarse fragment content (including gravel) and to develop regional datasets of soil texture for input. ~~Coarse fragment content affects soil physical properties. For example, soil porosity and saturated hydraulic conductivity are determined by the fraction of gravel, diameter and degree of mixture (Zhang et al., 2011).~~

Organic soil carbon content in mineral soil on the QTP affects soil porosity and thermal conductivity (Chen et al., 2012). ~~In~~ ~~However, in~~ the site considered in this study, the amount of organic soil carbon in soil was small (Figure 2), and we did not explicitly consider the effects of organic soil carbon on soil properties ~~explicitly~~. Alpine swamp meadow, alpine meadow, alpine steppe and alpine desert are the major vegetation types on the QTP (Wang et al., 2016; see also Figure 1b). Alpine swamp meadow and alpine meadow usually contain fine soil particles and high organic carbon density; while the other two types usually contain coarse soil particle and low organic carbon density (Qin et al., 2015). More laboratory work is needed to develop proper schemes for representing mixed soil with fine mineral, coarse fragment (including gravel), and organic carbon in permafrost models. It is the first priority to develop schemes that make use of porosity data sets, due to its importance and simplicity of measurement.

1 The development of a spatially explicit dataset of soil texture is also required for regional
2 ~~applications of projecting projections of~~ permafrost changes on the QTP. ~~One way is to collect~~
3 ~~relevant data through extensive field campaigns (e.g., Li et al., 2015).~~ Currently, ~~thea~~
4 ~~preliminary dataset considering gravel exists (Wu and Nan, 2016), though~~ gravelly soil has
5 only been mentioned in ~~scientific literature a few papers~~ on the QTP (Chen et al., 2015; Wang
6 et al., 2011; Yang et al., 2009). ~~Only recently, a preliminary dataset considering gravel has~~
7 ~~been created (Wu and Nan, 2016).~~ ~~One way to improve the regional dataset is to collect~~
8 ~~relevant data through extensive field campaigns (e.g. Li et al., 2015).~~ Ground penetrating
9 radar is a feasible tool to retrieve soil thickness above the coarse fragment soil layer (Han et
10 al., 2016). ~~), and coarse fragment soils can be identified in Aerial-aerial~~ photos taken with
11 unmanned aerial vehicles ~~have been used recently to identify coarse fragment soil~~ (Chen et al.,
12 2017; Yi 2017). In combination with ancillary datasets (e.g. geomorphology, topography,
13 vegetation), it is possible to improve the accuracy of spatial datasets of soil texture on the
14 QTP (Li et al., 2015; Wu et al., 2016). Another way is to retrieve soil physical properties
15 using data assimilation technology, such as Yang et al. (2016) who assimilated porosity using
16 a land surface model and microwave data.

17 5 Conclusions

18 In this study, we excavated soil samples from a permafrost site on the central QTP and
19 measured soil physical properties in laboratory. Coarse fragments ~~soils was were~~ common in
20 the soil profile (~~up to 65% of soil mass~~) and porosity was much smaller than the typical soil
21 types used in land surface models. We then performed sensitivity analysis of these parameters
22 on soil thermal and hydrological processes within a terrestrial ecosystem model. When default
23 sand or loam parameters were substituted with measured soil properties, the model errors of
24 ~~soil temperature, soil liquid water content, active layer depth and permafrost low boundary~~
25 were ~~generally~~ reduced by 74% or 84%, respectively. ~~Those of permafrost low boundary were~~
26 ~~reduced 35% or 34%, respectively.~~ Sensitivity analyses showed that porosity played a more
27 important role in reducing model errors than other soil properties examined. Though it is
28 unclear how representative this soil is in the QTP, it is clear that soil physical properties
29 specific to the QTP should be used to properly project permafrost dynamics into the future.

1 *Acknowledgements.* We would like to thank Prof. Dave McGuire of University of Alaska
2 Fairbanks for his careful editing; Dr. Yi Sun for vegetation classification; Dr. Xia Cui of
3 Lanzhou University, Mr. Guangyue Liu for determining depth of zero annual amplitude and
4 Mr. Yan Qin for measurements of soil particle size distribution; Prof. Chien-Lu Ping of
5 University of Alaska and Dr. Wangping Li of Lanzhou University of Technology for helping
6 on soil taxonomy; and the editor and two anonymous reviewers for valuable comments. This
7 study was jointly supported through grants provided as part of the National Natural Science
8 Foundation Commission (41422102, 41730751 and 41690142), [and the independent grants](#)
9 [from the State Key Laboratory of Cryosphere Sciences \(SKLCS-ZZ-2018\).](#)-

10 **References**

- 11 Anisimov, O. A.: Potential feedback of thawing permafrost to the global climate system
12 through methan emission, *Environ. Res. Lett.*, 2, 045016, doi:10.1088/1748-
13 9326/2/4/045016, 2007.
- 14 Arocena, J., K. Hall, and L.P.: Zhu Soil formation in high elevation and permafrost areas in
15 the Qinghai Plateau (China), *Spanish Journal of Soil Sciences*, 2, 34-49, 2012.
- 16 Azam, G., Grant, C. D., Murray, R. S., Nuberg, I. K., and Misra, R. K. : Comparison of the
17 penetration of primary and lateral roots of pea and different tree seedlings growing in
18 hard soils. *Soil Research*, 52, 87-96, 2014.
- 19 Boike, J., Kattenstroth, B., Abramova, E., Bornemann, N., Chetverova, A., Fedorova, I., and
20 Langer, M.: Baseline characteristics of climate, permafrost and land cover from a new
21 permafrost observatory in the Lena River Delta, Siberia (1998-2011), *Biogeosciences*
22 (BG), 10, 2105-2128, 2013.
- 23 Chen, H., Nan, Z., Zhao, L., Ding, Y., Chen, J., & Pang, Q.: Noah Modelling of the
24 Permafrost Distribution and Characteristics in the West Kunlun Area, Qinghai-Tibet
25 Plateau, China. *Permafrost Periglac*, 26,160-174, 2015.
- 26 Chen, J., Yi, S., and Qin, Y.: The contribution of plateau pika disturbance and erosion on
27 patchy alpine grassland soil on the Qinghai-Tibetan Plateau: Implications for grassland
28 restoration. *Geoderma*, 297, 1-9, 2017.
- 29 Chen, Y., Yang, K., Tang, W., Qin, J., and Zhao, L.: Parameterizing soil organic carbon's
30 impacts on soil porosity and thermal parameters for Eastern Tibet grasslands, *Science in*
31 *China Series D: Earth Sciences (EN)*, 55, 1001-1011, 2012.

1 Cote, J. and J. Konrad: A generalized thermal conductivity model for soils and construction
2 materials, *Can. Geotech. J.*, 42, 443-458, 2005.

3 Du, Z., Y. Cai, Y. Yan, and X. Wang: Embedded rock fragments affect alpine steppe plant
4 growth, soil carbon and nitrogen in the northern Tibetan Plateau, *Plant Soil*, 420, 79-92,
5 2017.

6 Farouki, O. T.: Thermal properties of soils, Cold Reg. Res. and Eng. Lab., Hanover, N. H,
7 1986.

8 Fox, J. D.: Incorporating Freeze-Thaw Calculations into a water balance model, *Water Resour.*
9 *Res.*, 28, 2229-2244, 1992.

10 Frey, K. E., and McClelland, J. W.: Impacts of permafrost degradation on arctic river
11 biogeochemistry, *Hydrol. Process*, 23, 169-182, 2009.

12 Goodrich, E. L.: Efficient Numerical Technique for one-dimensional Thermal Problems with
13 phase change, *Int. J. Heat Mass Transfer*, 21, 615-621, 1978.

14 Gwenzi, W., Hinz, C., Holmes, K., Phillips, I. R., and Mullins, I. J.: Field-scale spatial
15 variability of saturated hydraulic conductivity on a recently constructed artificial
16 ecosystem, *Geoderma*, 166, 43-56, 2011.

17 Han, X., Liu, J., Zhang, J., and Zhang, Z.: Identifying soil structure along headwater
18 hillslopes using ground penetrating radar based technique. *Journal of Mountain*
19 *Science*, 13, 405-415, 2016.

20 Jorgenson, M. T., Shur, Y. L., and Pullman, E. R.: Abrupt increase in permafrost degradation
21 in Arctic Alaska, *Res. Lett.*, 33, L02503, doi:10.1029/2005GL024960, 2006.

22 Langer, M., Westermann, S., Heikenfeld, M., Dorn, W., and Boike, J.: Satellite-based
23 modeling of permafrost temperatures in a tundra lowland landscape, *Remote Sensing of*
24 *Environment*, 135, 12-24, 2013.

25 Li, J., Sheng, Y., Wu, J., Chen, J., and Zhang, X.: Probability distribution of permafrost along
26 a transportation corridor in the northeastern Qinghai province of China. *Cold Regions*
27 *Science and Technology*, 59, 12-18, 2009.

28 Li, W., L. Zhao, X. Wu, Y. Zhao, H. Fang, and W. Shi: Distribution of soils and landform
29 relationships in the permafrost regions of Qinghai-Xizang (Tibetan) Plateau, *Chinese Sci.*
30 *Bull.*, 23, 2216-2226, 2015.

31 Lin, Z., F. Niu, H. Liu, and J. Lu: Hydrothermal processes of alpine tundra lakes, Beiluhe
32 Basin, Qinghai-Tibet Plateau, *Cold Reg. Sci. Technol.*, 65, 446-455, 2011.

- 1 Luo, S., Lv, S., Zhang, Y., Hu, Z., Ma, Y., Li, S., and Shang, L.: Soil thermal conductivity
2 parameterization establishment and application in numerical model of central Tibetan
3 Plateau, Chinese Journal of Geophysics, 52, 919-928, 2009. (in Chinese with English
4 Abstract)
- 5 McGuire, A. D., J. Melillo, E. G. Jobbagy, D. Kicklighter, A. L. Grace, B. Moore, and C. J.
6 Vorosmarty: Interactions Between Carbon and Nitrogen Dynamics in Estimating Net
7 Primary Productivity for Potential Vegetation in North America, Global Biogeochem. Cy.,
8 6(2), 101-124, 1992.
- 9 McGuire, A. D., J. S. Clein, J. Melillo, D. Kicklighter, R. A. Meier, C. J. Vorosmarty, and M.
10 C. Serreze: Modelling carbon responses of tundra ecosystems to historical and projected
11 climate: sensitivity of pan-Arctic carbon storage to temporal and spatial variation in
12 climate, Global Change Biol., 6 (Suppl. 1), 141-159, 2000.
- 13 McGuire, A. D., Anderson, L. G., Christensen, T. R., Dallimore, S., Guo, L., Hayes, D. J., .
14 and Roulet, N.: Sensitivity of the carbon cycle in the Arctic to climate change. Ecological
15 Monographs, 79, 523-555, 2009.
- 16 Nan, Z., Li, S., and Cheng, G.: Prediction of permafrost distribution on the Qinghai-Tibet
17 Plateau in the next 50 and 100 years. Science in China Series D: Earth Sciences, 48, 797-
18 804, 2005.
- 19 Nelson, F. E., Anisimov, O. A., and Shiklomanov, N. I.: Subsidence risk from thawing
20 permafrost, Nature, 410(6831), 889-890, 2001.
- 21 Oleson, K. W., Lawrence, D. M., Bonan, G. B., Flanner, M. G., Kluzek, E., Lawrence, P. J.,
22 Levis, S., Swenson, S. C., and Thornton, P.: Technical description of version 4.0 of the
23 Community Land Model (CLM), University Corporation for Atmospheric Research,
24 NCAR 2153-2400, 2010.
- 25 Pan, Y., S. Lv, S. Li, Y. Gao, X. Meng, Y. Ao, and S. Wang: Simulating the role of gravel in
26 freeze-thaw process on the Qinghai-Tibet Plateau, Theor. Appl. Climatol., 127, 1011-
27 1022, 2017.
- 28 ~~Qin, Y., J. E. Hiller, G. Jiang, and T. Bao: Sensitivity of thermal parameters affecting cold-~~
29 ~~region ground temperature predictions, Environ. Earth Sci., 68, 1757-1772, 2013.~~
- 30 Qin, Y., Yi, S., Chen, J., Ren, S., and Ding, Y.: Effects of gravel on soil and vegetation
31 properties of alpine grassland on the Qinghai-Tibetan plateau. Ecological Engineering, 74,
32 351-355, 2015.

- 1 Qin Y., Wu, T. , Zhao, L., Wu, X., Li, R., Xie, C., Pang, Q., Hu, G., Qiao, Y., Zhao, G., Liu,
2 G., Zhu, X., and Hao, J.: Numerical Modeling of the Active Layer Thickness and
3 Permafrost Thermal State Across Qinghai-Tibetan Plateau, *Journal of Geophysical*
4 *Research: Atmospheres*, doi:10.1002/2017JD026858, 2017.
- 5 ~~Qin, Y., S. Yi, Y. Ding, G. Xu, J. Chen, and Z. Wang: Effects of small scale patchiness of~~
6 ~~alpine grassland on ecosystem carbon and nitrogen accumulation and estimation in~~
7 ~~northeastern Qinghai-Tibetan Plateau, *Geoderma*, 318, 52-63, 2018.~~
- 8 Romanovsky, V. E. and T. E. Osterkamp: Effects of unfrozen water on heat and mass
9 transport processes in the active layer and permafrost, *Permafrost Periglac.*, 11, 219-239,
10 2000.
- 11 Salmon, V. G., Soucy, P., Mauritz, M., Celis, G., Natali, S. M., Mack, M. C., and Schuur, E.
12 A.: Nitrogen availability increases in a tundra ecosystem during five years of
13 experimental permafrost thaw, *Global Change Biol.*, 22, 1927-1941, 2016.
- 14 Soil Survey Staff. *Keys to Soil Taxonomy*, 12th ed. USDA-Natural Resources Conservation
15 Service, Washington, DC, 2014.
- 16 ~~Stephens, D. B., K. Hsu, M. A. Prieksat, M. D. Ankeny, N. Blandford, T. L. Roth, J. A.~~
17 ~~Kelsey, and J. R. Whitworth: A comparison of estimated and calculated effective porosity,~~
18 ~~*Hydrol. Process*, 6, 156-165, 1998.~~
- 19 Swenson, S. C., D. M. Lawrence, and H. Lee: Improved simulation of the terrestrial
20 hydrological cycle in permafrost regions by the Community Land Model, *Journal of*
21 *Advances in Modeling Earth Systems*, 4, M08002, doi:10.1029/2012MS000165, 2013.
- 22 Walvoord, M. A., and Striegl, R. G.: Increased groundwater to stream discharge from
23 permafrost thawing in the Yukon River basin: Potential impacts on lateral export of
24 carbon and nitrogen. *Geophys. Res. Lett.*, 34, L12402, doi:10.1029/2007GL030216, 2007.
- 25 Wang, F. X., Kang, Y., Liu, S. P., and Hou, X. Y.: Effects of soil matric potential on potato
26 growth under drip irrigation in the North China Plain. *Agricultural water management*, 88,
27 34-42, 2007.
- 28 Wang, G., Li. Y., Wang. Y., and Wu, Q.: Effects of permafrost thawing on vegetation and soil
29 carbon pool losses on the Qinghai-Tibet Plateau, China, *Geoderma*, 143, 143-152,2008.
- 30
- 31 Wang, H., B. Xiao, M. Wang, and Ming'an Shao: Modeling the soil water retention curves of
32 soil-gravel mixtures with regression method on the Loess Plateau of China, *PLoS ONE*, 8,
33 e59475, doi:10.1371/journal.pone.0059475, 2013.

- 1 Wang, L., Zhou, J., Qi, J., Sun, L., Yang, K., Tian, L., and Koike, T.: Development of a land
2 surface model with coupled snow and frozen soil physics, *Water Resources Research*, 53,
3 5085-5103, doi:10.1002/2017WR020451, 2017.
- 4 Wang, X., Liu, G., and Liu, S.: Effects of gravel on grassland soil carbon and nitrogen in the
5 arid regions of the Tibetan Plateau. *Geoderma*, 166, 181-188, 2011.
- 6 Wang, Z., Q. Wang, L. Zhao, X. Wu, G. Yue, D. Zou, Z. Nan, G. Liu, Q. Pang, H. Fang, T.
7 Wu, J. Shi, K. Jiao, Y. Zhao, and L. Zhang: Mapping the vegetation distribution of the
8 permafrost zone on the Qinghai-Tibet Plateau, *Journal of Mountain Sciences*, 13, 1035-
9 1046, 2016.
- 10 Woo, M. K., Arain, M. A., Mollinga, M., and Yi, S.: A two-directional freeze and thaw
11 algorithm for hydrologic and land surface modelling. *Geophys. Res. Lett.*, 31, L12501,
12 doi:10.1029/2004GL019475, 2004.
- 13 Wright, N., Hayashi, M., and Quinton, W. L.: Spatial and temporal variations in active layer
14 thawing and their implication on runoff generation in peat-covered permafrost
15 terrain. *Water Resour. Res.*, 45, W05414, doi:10.1029/2008WR006880, 2009.
- 16 Wu, Q., Cheng, G., and Ma, W.: Impact of permafrost change on the Qinghai-Tibet Railroad
17 engineering. *Science in China Series D: Earth Sciences*, 47, 122-130, 2004.
- 18 Wu, Q., and Zhang, T.: Changes in active layer thickness over the Qinghai-Tibetan Plateau
19 from 1995 to 2007. *J. Geophys. Res.*, 115, D09107, doi:10.1029/2009JD012974, 2010.
- 20 Wu, Q., Z. Zhang, S. Gao, and W. Ma: Thermal impacts of engineering activities and
21 vegetation layer on permafrost in different alpine ecosystems of the Qinghai-Tibet
22 Plateau, China, *The Cryosphere*, 10, 1695-1706, 2016.
- 23 Wu, X., Zhao, L., Fang, H., Zhao, Y., Smoak, J. M., Pang, Q., and Ding, Y.: Environmental
24 controls on soil organic carbon and nitrogen stocks in the high-altitude arid western
25 Qinghai-Tibetan Plateau permafrost region, *J. Geophys. Res.*, 121, 176-187, 2016.
- 26 Wu, X. and Nan, Z.: A Multilayer Soil Texture Dataset for Permafrost Modeling over
27 Qinghai– Tibetan Plateau, *IGARSS*, 4917-4920, 2016
- 28
- 29 Wu, X., Z. Nan, S. Zhao, L. Zhao, and G. Cheng: Spatial modeling of permafrost distribution
30 and properties on the Qinghai-Tibetan Plateau, *Permafrost Periglac.*, DOI:
31 10.1002/ppp.1971, 2018

带格式的: 段落间距段前: 6 磅

- 1 Yang, J., Mi, R., and Liu, J.: Variations in soil properties and their effect on subsurface
2 biomass distribution in four alpine meadows of the hinterland of the Tibetan Plateau of
3 China, *Environ. Geol.*, 57, 1881-1891, 2009.
- 4 Yang, K., Zhu, L., Chen, Y., Zhao, L., Qin, J., Lu, H., . and Fang, N.: Land surface model
5 calibration through microwave data assimilation for improving soil moisture
6 simulations, *Journal of Hydrology*, 533, 266-276, 2016.
- 7 Ye, B., Yang, D., Zhang, Z., and Kane, D. L.: Variation of hydrological regime with
8 permafrost coverage over Lena Basin in Siberia. *J. Geophys. Res.*, 114, D07102,
9 doi:10.1029/2008JD010537, 2009.
- 10 Yi, S., Manies, K. L., Harden, J., and McGuire, A. D.: The characteristics of organic soil in
11 black spruce forests: Implications for the application of land surface and ecosystem
12 models in cold regions, *Geophys. Res. Lett.*, 36, L05501, doi:10.1029/2008GL037014,
13 2009a.
- 14 Yi, S., McGuire, A. D., Harden, J., Kasischke, E., Manies, K. L., Hinzman, L. D., Liljedahl,
15 A., Randerson, J. T., Liu, H., Romanovsky, V. E., Marchenko, S., and Kim, Y.:
16 Interactions between soil thermal and hydrological dynamics in the response of Alaska
17 ecosystems to fire disturbance , *J. Geophys. Res.*, 114, G02015,
18 doi:10.1029/2008JG000841, 2009b.
- 19 Yi, S., McGuire, A. D., Kasischke, E., Harden, J., Manies, K. L., Mack, M., and Turetsky, M.
20 R.: A Dynamic organic soil biogeochemical model for simulating the effects of wildfire
21 on soil environmental conditions and carbon dynamics of black spruce forests, *J.*
22 *Geophys. Res.*, 115, G04015, doi:10.1029/2010JG001302, 2010.
- 23 Yi. S., Li, N., Xiang, B., Ye, B. and McGuire, A.D.: Representing the effects of alpine
24 grassland vegetation cover on the simulation of soil thermal dynamics by ecosystem
25 models applied to the Qinghai-Tibetan Plateau, *J. Geophys. Res.*, 118, 1-14, doi:
26 10.1002/jgrg.20093, 2013.
- 27 Yi, S., Wang, X., Qin, Y., Xiang, B., and Ding, Y.: Responses of alpine grassland on
28 Qinghai-Tibetan plateau to climate warming and permafrost degradation: a modeling
29 perspective. *Environ. Res. Lett.*, 9, 074014, doi:10.1088/1748-9326/9/7/074014, 2014a.
- 30 Yi, S., Wischniewski, K., Langer, M., Muster, S., Boike, J.: Modeling different freeze/thaw
31 processes in heterogeneous landscapes of the Arctic polygonal tundra using an ecosystem
32 model. *Geoscientific Model Development*, 7, 1671-1689, 2014b.

1 Yi S, FragMAP: a tool for long-term and cooperative monitoring and analysis of small-scale
2 habitat fragmentation using an unmanned aerial vehicle, *International Journal of Remote*
3 *Sensing*, 38:2686-2697, 2017.

4 Yin, G., Niu, F., Lin, Z., Luo, J., and Liu, M.: Effects of local factors and climate on
5 permafrost conditions and distribution in Beiluhe basin, Qinghai-Tibet Plateau, China.
6 *Science of the Total Environment*, 581-582, 472-485, 2017.

7 Yuan, F. M., Yi, S. H., McGuire, A. D., Johnson, K. D., Liang, J., Harden, J. W., ... and Kurz,
8 W. A.: Assessment of boreal forest historical C dynamics in the Yukon River Basin:
9 relative roles of warming and fire regime change *Ecol, Appl.*, 22, 2091-2109, 2012.

10 Zhang, Z. F., and Ward, A. L.: Determining the porosity and saturated hydraulic conductivity
11 of binary mixtures, *Vadose Zone J.*, 10, 313-321, 2011.

12 Zhuang, Q., V. E. Romanovsky, and A. D. McGuire: Incorporation of a permafrost model into
13 a large-scale ecosystem model: Evaluation of temporal and spatial scaling issues in
14 simulating soil thermal dynamics, *J. Geophys. Res.*, 106(D24), 33649-33670, 2001.

15 Zhuang, Q., J. Melillo, D. Kicklighter, R. G. Prinn, A. D. McGuire, P. A. Steudler, B. S.
16 Felzer, and S. Hu: Methane fluxes between terrestrial ecosystems and the atmosphere at
17 northern high latitudes during the past century: A retrospective analysis with a process-
18 based biogeochemistry model, *Global Biogeochem. Cy.*, 18, GB3010,
19 doi:10.1029/2004GB002239, 2004.

20 Zhuang, Q., J. He, Y. Lu, L. Ji, J. Xiao, and T. Luo: Carbon dynamics of terrestrial
21 ecosystems on the Tibetan Plateau during the 20th century: an analysis with a process-
22 based biogeochemical model, *Global Ecol. Biogeogr.*, 19, 649-662, 2010.

23 Zou, D., L. Zhao, Y. Sheng, J. Chen, G. Hu, T. Wu, J. Wu, C. Xie, X. Wu, Q. Pang, W. Wang,
24 E. Du, W. Li, G. Liu, J. Li, Y. Qin, Y. Qiao, Z. Wang, J. Shi, and G. Cheng: A new map
25 of permafrost distribution on the Tibetan Plateau, *The Cryosphere*, 11, 2527-2542, 2017.

26

1 **Table 1.** The mean (standard deviation in brackets) of measured soil bulk density ($\rho_b, \text{g cm}^{-3}$)
 2 ρ_b , calculated porosity from bulk density ($\phi_c, \text{m}^3 \text{m}^{-3}$), measured porosity ($\phi_m, \text{m}^3 \text{m}^{-3}$) of
 3 different layers based on soil samples in this study.

- 带格式的：下标
- 带格式的：上标
- 带格式的：下标
- 带格式的：上标
- 带格式的：上标

Layer (cm)	Bulk density (g cm^{-3}) ρ_b	ϕ_c Calculated Porosity (%)	Measured porosity (%) ϕ_m
0—10	1.74 (0.21)	34.4 (0.08)	28.4 (0.03)
10—20	1.81 (0.11)	31.8 (0.04)	27.7 (0.02)
20—30	1.86 (0.32)	29.7 (0.12)	30.2 (0.05)
40—50	1.61 (0.23)	39.4 (0.09)	29.6 (0.02)
70—80	1.62 (0.20)	38.8 (0.08)	20.6 (0.11)
110—120	1.75 (0.09)	33.9 (0.04)	27.7 (0.01)
150—160	1.70 (0.15)	36.0 (0.06)	26.3 (0.02)
190—200	1.81 (0.09)	31.6 (0.03)	27.1 (0.02)

5

1 **Table 2.** The particle size diameter fractions (for >2 mm this is the mass ratio between soil
 2 particles greater than 2 mm and total soil sample, while for the other fractions this is the ratio
 3 between mass of the soil in the size range and the mass of all particles < 2mm) and soil
 4 texture (based on USDA classification) of different layers based on soil samples in this study.
 5

Layer (cm)	>2 mm	<u>>2mm -</u> 63 μ m	<u>2-63-2</u> μ m	<2 μ m	Texture
0—10	0.38 (0.07)	0.77 (0.07)	0.18 (0.04)	0.05 (0.02)	Loamy sand
10—20	0.52 (0.14)	0.72 (0.11)	0.20 (0.05)	0.07 (0.05)	Loamy sand
20—30	0.55 (0.17)	0.69 (0.09)	0.24 (0.08)	0.07 (0.01)	Sandy loam
40—50	0.55 (0.19)	0.70 (0.13)	0.26 (0.11)	0.04 (0.02)	Loamy sand
70—80	0.65 (0.16)	0.71 (0.09)	0.25 (0.07)	0.04 (0.02)	Loamy sand
110—120	0.63 (0.05)	0.79 (0.09)	0.19 (0.08)	0.03 (0.02)	Loamy sand
150—160	0.63 (0.09)	0.85 (0.04)	0.13 (0.03)	0.02 (0.01)	Loamy sand
190—200	0.50 (0.19)	0.71 (0.19)	0.24 (0.14)	0.05 (0.05)	Loamy sand

6
7
8

1 **Table 3.** The mean (standard deviation in brackets) of the measured frozen and unfrozen dry
 2 and saturated soil thermal conductivity ($\text{W m}^{-1} \text{K}^{-1}$) of different soil layers.

3

Layer (cm)	Dry		Saturated	
	Unfrozen	Frozen	Unfrozen	Frozen
0-10	0.238 (0.09)	0.414 (0.09)	2.322 (0.17)	3.122 (0.48)
10~20	0.340 (0.04)	0.365 (0.23)	2.147 (0.47)	3.193 (0.55)
20-30	0.395 (0.07)	0.420 (0.11)	2.743 (0.38)	3.059 (0.29)
40-50	0.346 (0.00)	0.388 (0.14)	2.539 (0.30)	3.184 (0.33)
70-80	0.340 (0.03)	0.289 (0.12)	2.589 (0.16)	3.362 (0.38)
110-120	0.400 (0.06)	0.271 (0.07)	2.616 (0.11)	3.721 (0.05)
150-160	0.401 (0.01)	0.248 (0.07)	2.246 (0.19)	3.647 (0.48)
190-200	0.399 (0.26)	0.392 (0.14)	2.609 (0.12)	3.329 (0.19)

4

5

1 **Table 4.** The mean (standard deviation) of measured saturated hydraulic conductivity (K_{sat} ;
 2 mm s^{-1}) and fitted absolute value of saturated matric potential (Ψ_{sat} ; mm), fitted pore size
 3 distribution parameter (B) and the correlation coefficients (R^2) between calculated matric
 4 potential using fitted equations and measured.

5

Layer (cm)	K_{sat}	Matric potential		
		Ψ_{sat}	B	R^2
0-10	0.0285 (0.0274)	49.14	4.03	0.991
10~20	0.0056 (0.0036)	70.66	4.49	0.996
20-30	0.0047 (0.0027)	27.02	5.22	0.994
40-50	0.0078 (0.0043)	143.4	3.59	0.994
70-80	0.0072 (0.0054)	179.6	3.22	0.993
110-120	0.0315 (0.0054)	603.7	1.89	0.969
150-160	0.0053 (0.0028)	49.17	2.97	0.993
190-200	0.0036 (0.0023)	14.47	4.565	0.989

6

7

1 **Table 5.** Model performance when default sand parameters are substituted with combinations
 2 of measured porosity (I), thermal conductivity (II), hydraulic conductivity (III) and matric
 3 potential (IV).

	Best	I	II	III	IV	V	VI	VII	VIII	IX	X	All
	II	III	V	III	IV	III	II	II	III	III		
						V	III	IV	IV	IV		
100 cm ST	II											
ALD	I	1										
PLB	II	1	2									
10 cm SM	I	7	2	4			1	5	6			3
40 cm SM	I											
80 cm SM	I	7	1	4			2	6	5			3
160 cm CM	I	1										

4 **Note:** Best column shows the model simulations (individual parameter substitution) with the
 5 smallest root mean squared error (RMSE) for 100 cm soil temperature (ST, °C), active layer
 6 depth (ALD, m), permafrost low boundary (PLB, m), 10, 40, 80 and 160 cm soil liquid water
 7 content (SM, -); Numbers indicate the combination of parameters that have smaller RMSE
 8 than the best model run using individual parameter substitution. “All” indicates the
 9 combination of all 4 parameters. The smallest number indicates the smallest RMSE.

10
 11
 12
 13

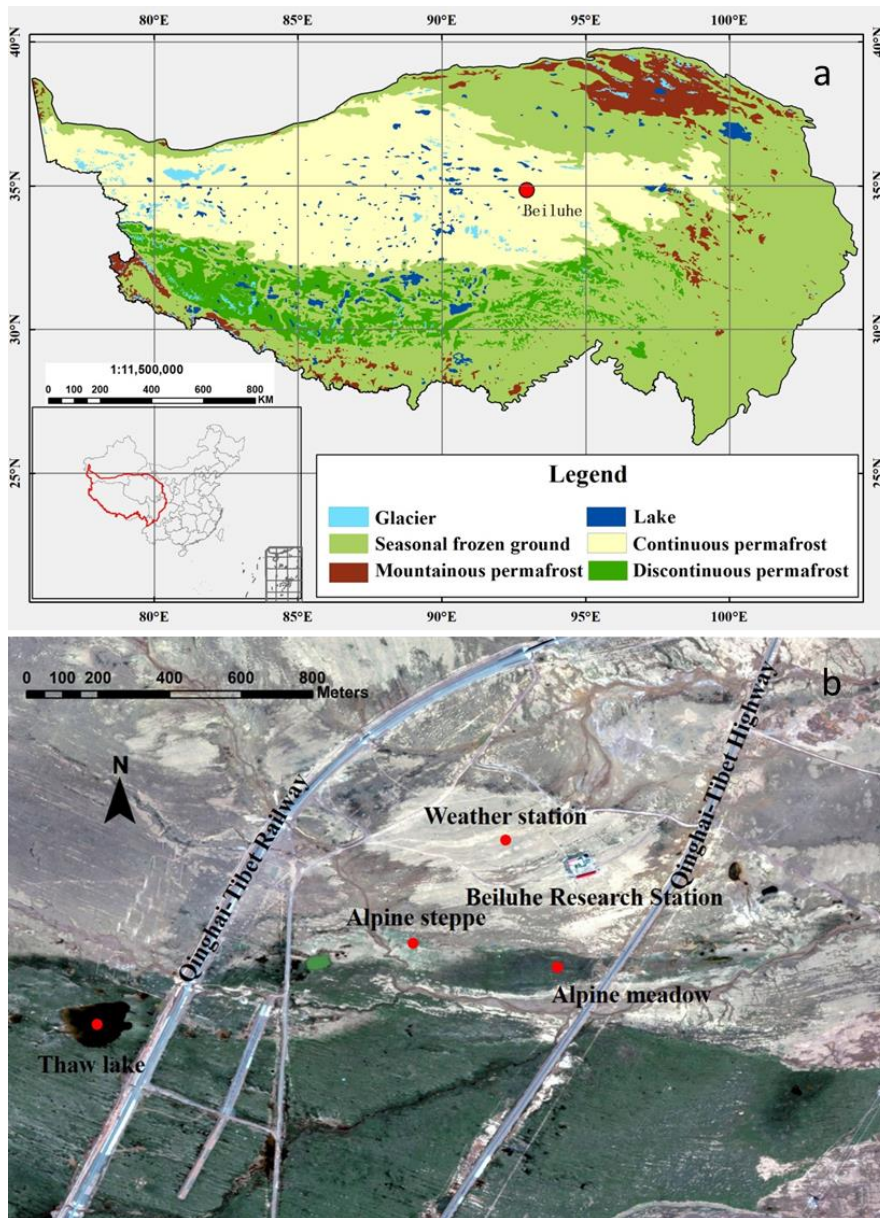
1 **Table 6** Model performance when default loam parameters are substituted with combinations
 2 of measured porosity (I), thermal conductivity (II), hydraulic conductivity (III) and matric
 3 potential (IV) .

4

	Best	I	I	I	II	II	I	I	I	I	II	All
		II	III	IV	III	IV	III	II	II	III	III	
							V	III	IV	IV	IV	
100 cm ST	I	1		2					3			
ALD	I	3	5					1	2	6		4
PLB	II											
10 cm SM	I	7	6	1				5	2	4		3
40 cm SM	I	5	7	1				6	3	4		2
80 cm SM	I											
160 cm SM	I	1	3					2				

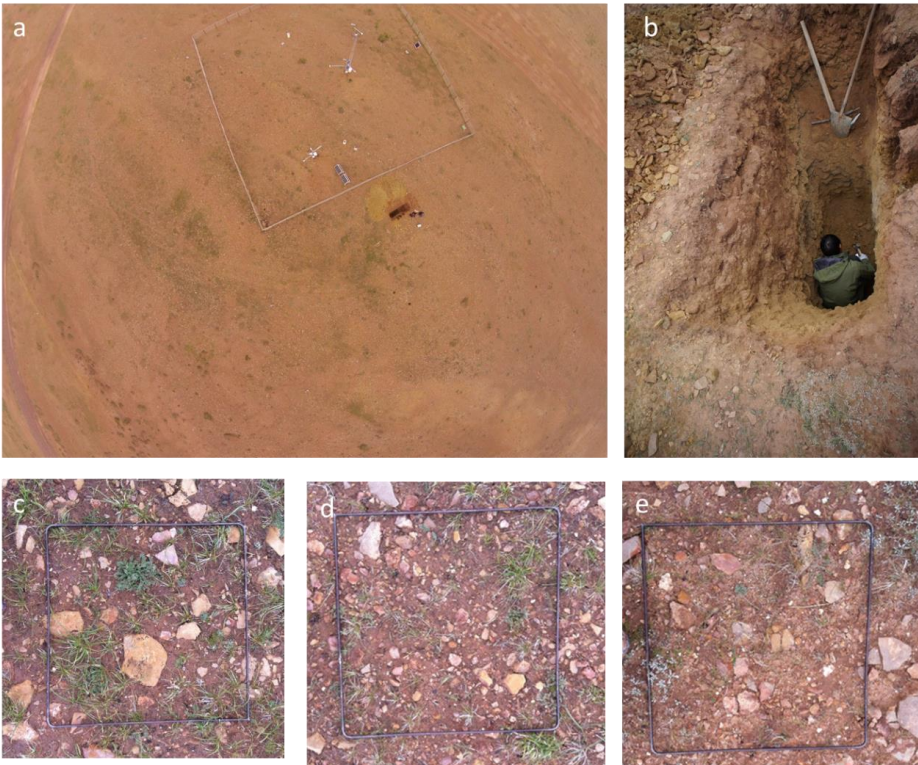
5
 6 **Note:** Best column shows the model simulations (individual parameter substitution) with the
 7 smallest root mean squared error (RMSE) for 100 cm soil temperature (ST, °C), active layer
 8 depth (ALD, m), permafrost low boundary (PLB, m), 10, 40, 80 and 160 cm soil liquid water
 9 content (SM, -); Numbers indicate the combination of parameters that have smaller RMSE
 10 than the best model run using individual parameter substitution. “All” indicates the
 11 combination of all 4 parameters. The smallest number indicates the smallest RMSE.

1 **Figure 1. a)** Locations of a) Beiluhe permafrost station on the Qinghai-Tibetan Plateau, and b)
2 ~~the googlemap of~~ the weather station and the surrounding environment (Map data: Google,
3 DigitalGlobe).



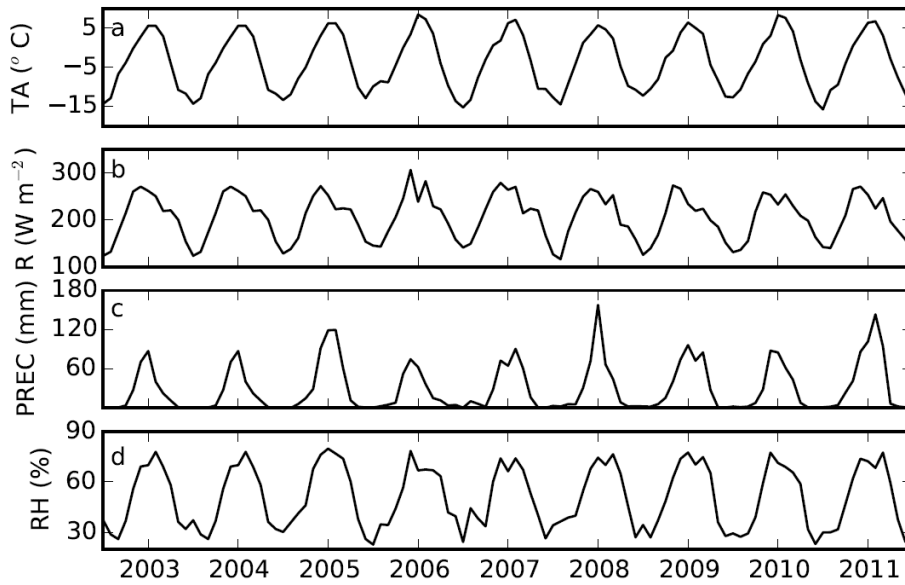
4
5

1 **Figure 2.** Images of site conditions: **a)** the aerial view of the weather station and the
2 excavated soil pit (the borehole is located in the lower left corner of white fence); **b)** the
3 detailed view of the excavated soil pit; and **c)-e)** examples of vegetation, gravel and stones
4 (iron frame is about 0.5 m×0.5 m).



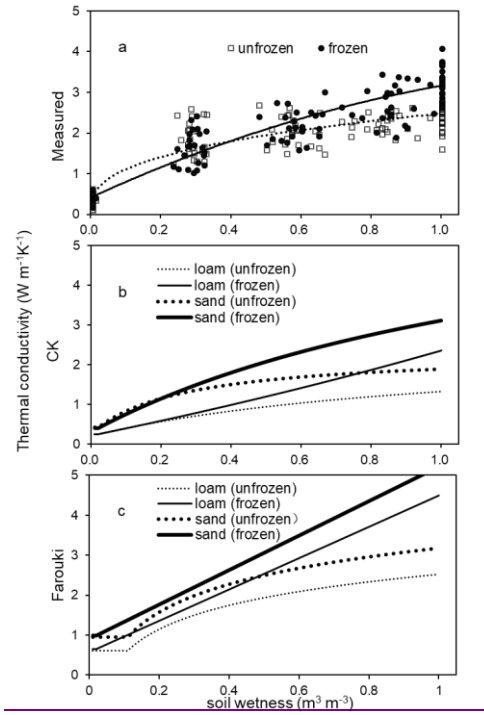
5
6
7
8

1 **Figure 3.** Time series of data measured at the Beiluhe weather station, Qinghai-Tibetan
2 Plateau, 2003 to 2011: **a)** air temperature (TA, °C); **b)** downward solar radiation (R, W m⁻²); **c)**
3 precipitation (PREC, mm); and **d)** relative humidity (RH, %).

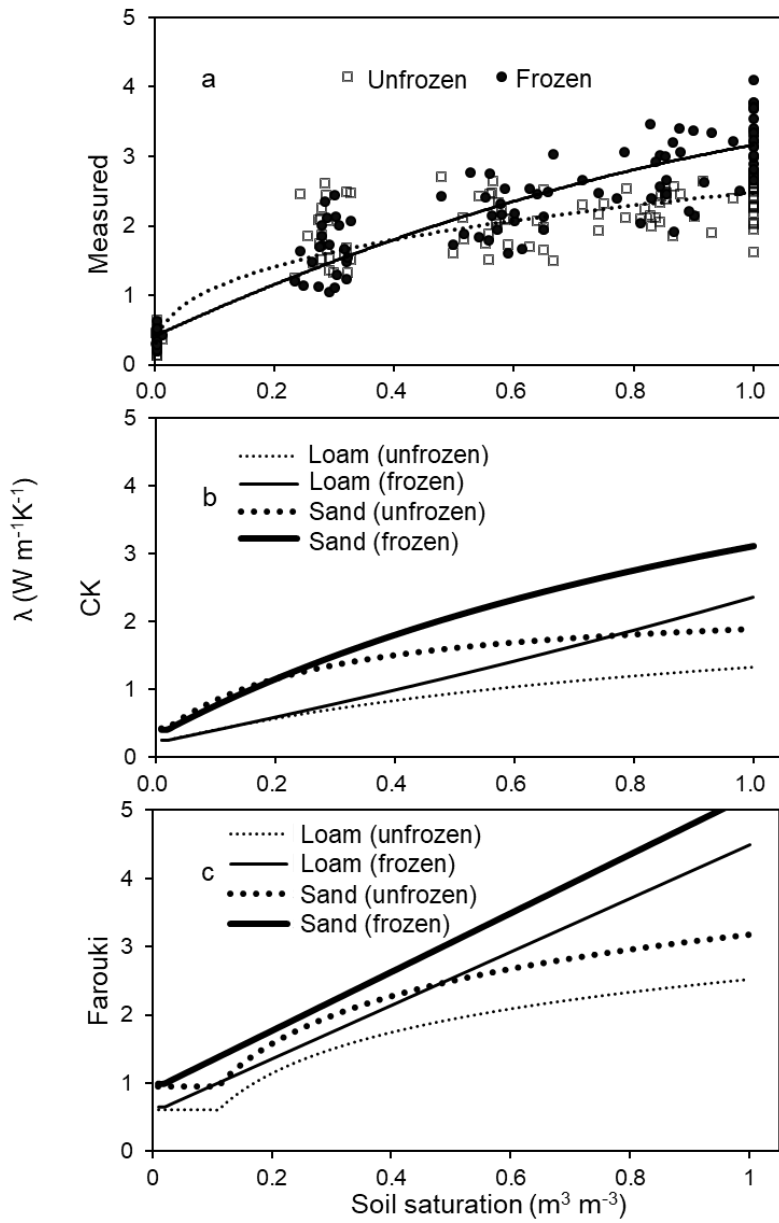


4

1 **Figure 4.** The relationship between soil wetness-saturation (solid and dotted lines represent
2 frozen and unfrozen cases) and soil thermal conductivity (λ_s , $\text{W m}^{-1}\text{K}^{-1}$) from: **a)** measured
3 values (Measured; dots and empty diamonds represent measured frozen and unfrozen soil
4 thermal conductivities, respectively); **b)** using the Côté and Konrad (2005) scheme (CK);
5 and **c)** using the Farouki (1986) scheme (Farouki). **Thick and thin lines represent relationships**
6 **for sand and loam, respectively.**



7

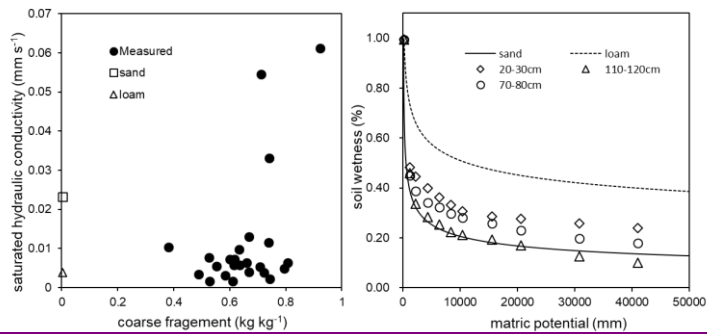


1
2

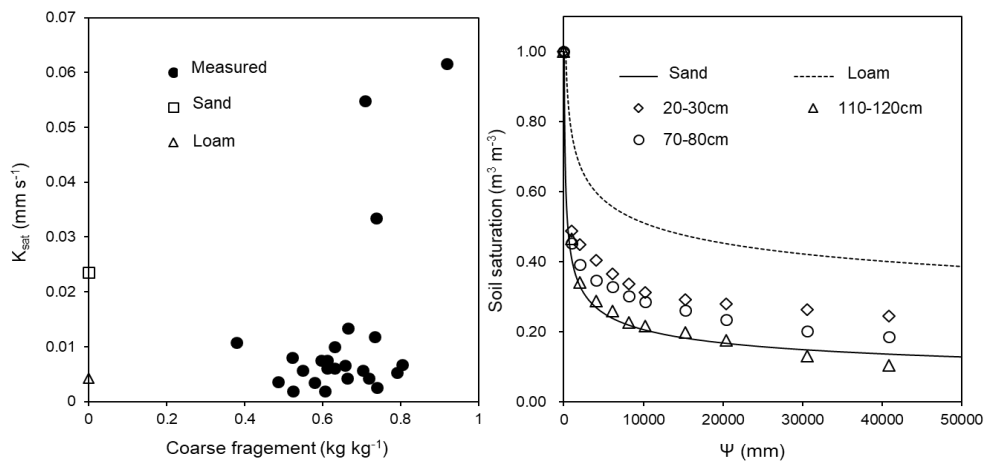
1 **Figure 5.** The relations between: a) saturated hydraulic conductivity (K_{sat} , mm s^{-1}) and coarse
 2 fragment fraction (Solid dots represent measured value; empty circle and empty triangle
 3 represent the corresponding values of sand and loam used in Community Land Model,
 4 respectively), and b) soil saturationwetness ($\text{m}^3 \text{m}^{-3}$, lines) and absolute value of matric
 5 potential (Ψ , $\text{mm H}_2\text{O}$) at three representative depths (-solid and dashed lines represent
 6 default values (Oleson et al., 2010) of sand and loam, respectively).

带格式的: 上标
 带格式的: 上标

7



8

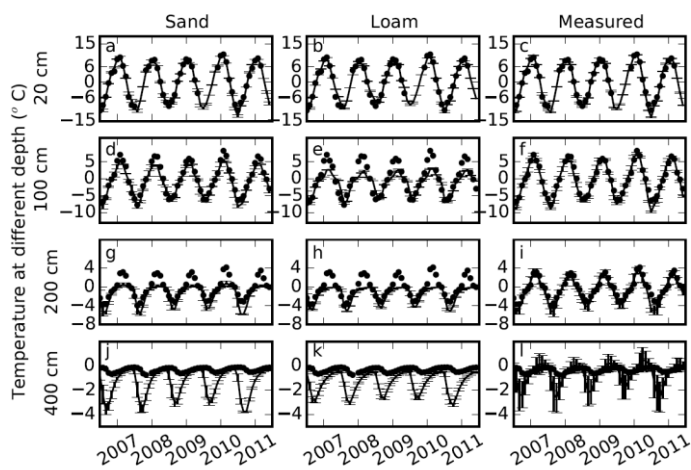


9

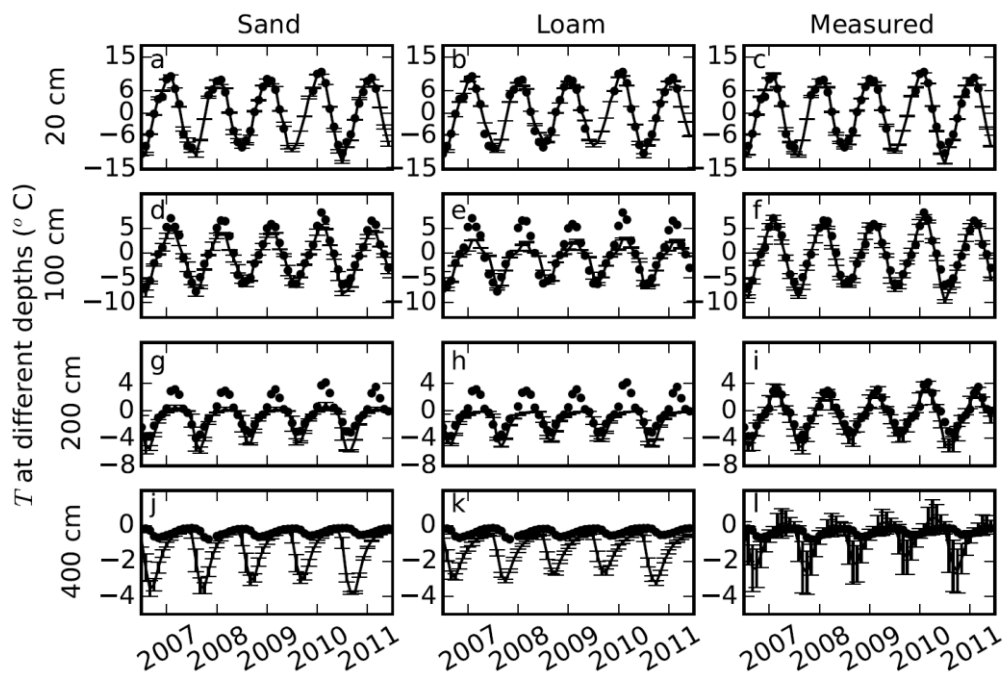
10

1 **Figure 6.** Comparisons of soil temperatures ($T, ^\circ\text{C}$) simulated using default parameters for
 2 sand, loam, and our measured parameters (lines) with measured soil temperatures (dots) at 20,
 3 100, 200, and 400 cm depths. Error bars show the standard deviations calculated based on 9
 4 simulations with 3 different slopes and 3 different soil thicknesses (Measured porosities were
 5 used in the simulation).

6



7

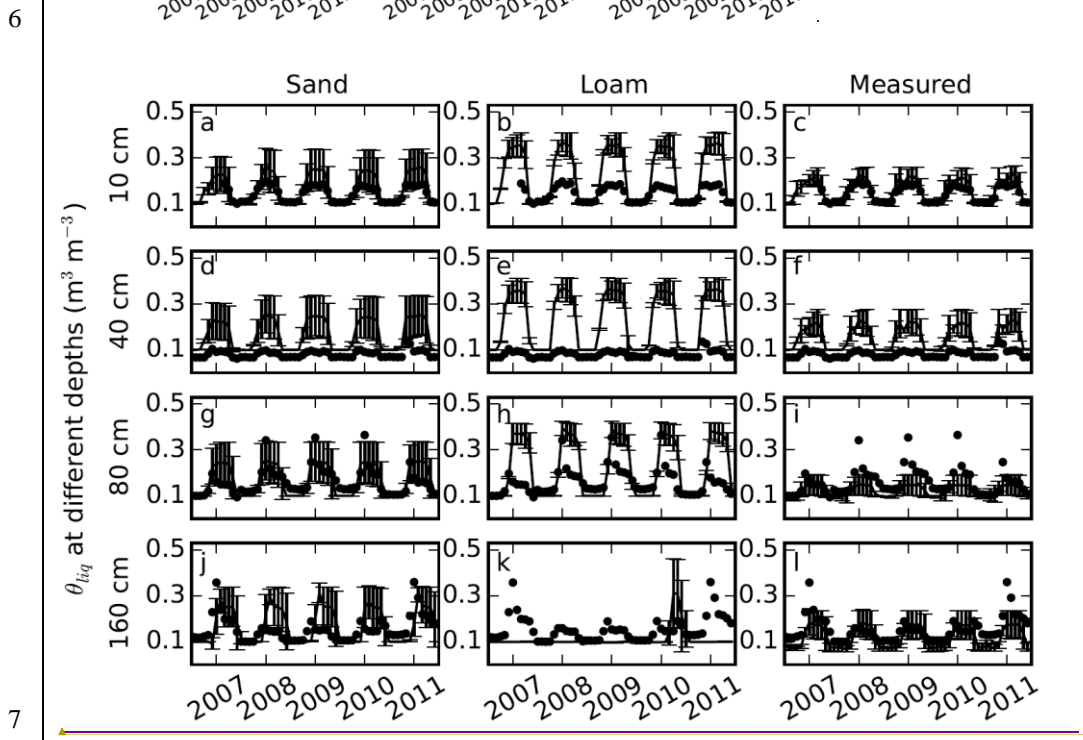


8

9

1 **Figure 7.** Comparisons of soil volumetric liquid water content (θ_{liq} in $m^3 m^{-3}$) simulated
 2 using default parameters sand, default loam, and measured parameters (lines) with measured
 3 soil moistures (dots) at 10, 40, 80, and 160 cm depths. Error bars showed the standard
 4 deviation calculated based on 9 simulations with 3 different slopes and 3 different soil
 5 thicknesses (Measured porosities were used in the simulation).

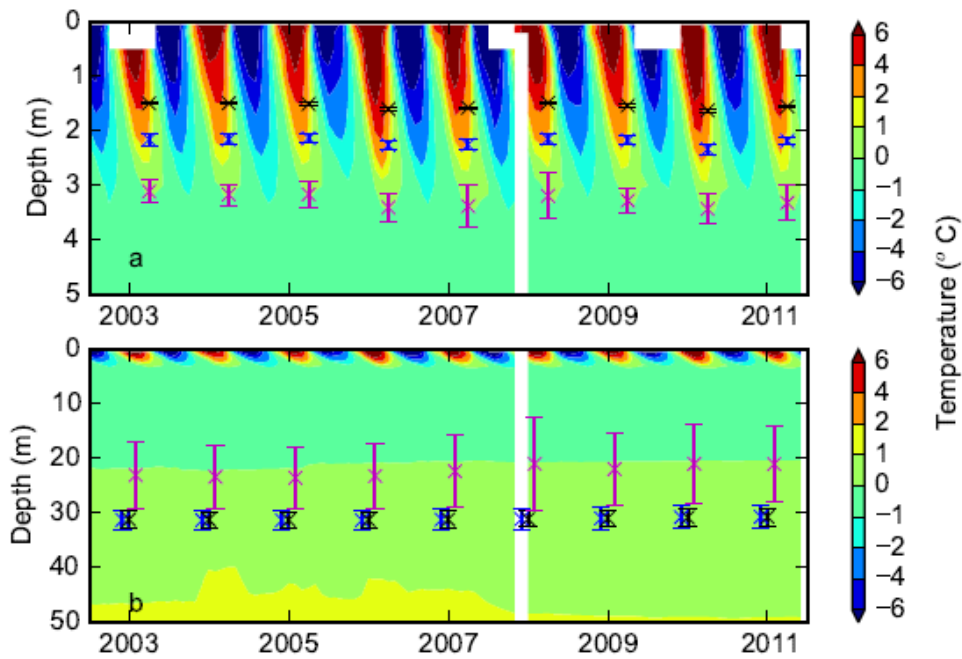
带格式的: 下标
 带格式的: 上标
 带格式的: 上标



带格式的: 字体颜色: 红色

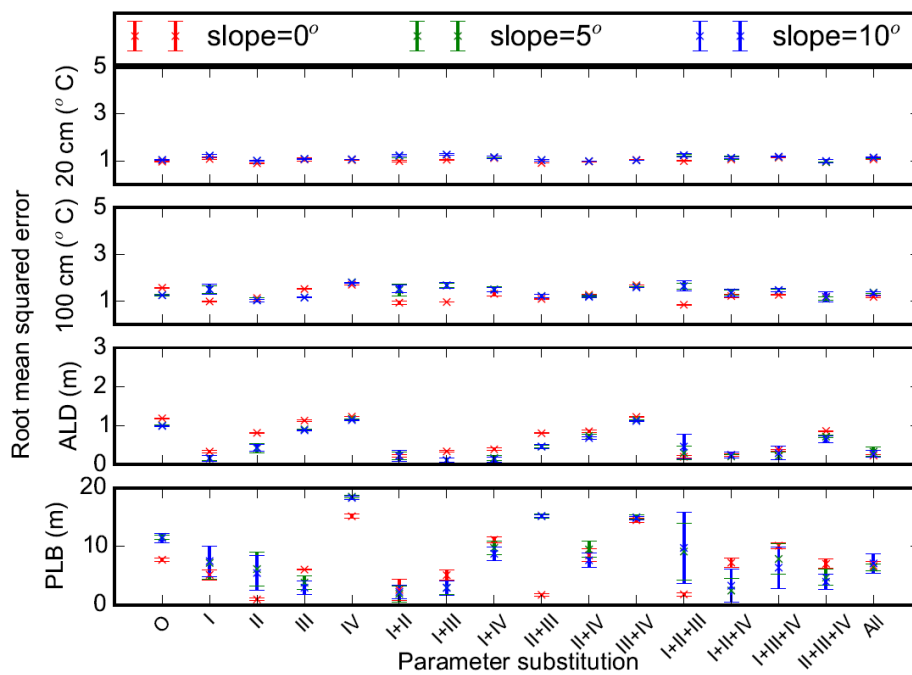
7
 8

1 **Figure 8.** Contour plots showing **a)** soil temperature ($^{\circ}\text{C}$) from borehole measurements down
2 to 5 m superimposed with simulated active layer depths over the period of 2003-2011; and **b)**
3 ground temperature down to 50 m superimposed with the simulated permafrost low boundary.
4 Black, blue and magenta represent simulations with loam, sand, and measured parameters,
5 respectively. Error bars show the standard deviation calculated based on 9 simulations with 3
6 different slopes and 3 different soil thicknesses (Measured porosities were used in the
7 simulation. White zones in the contour plots indicate missing borehole data).



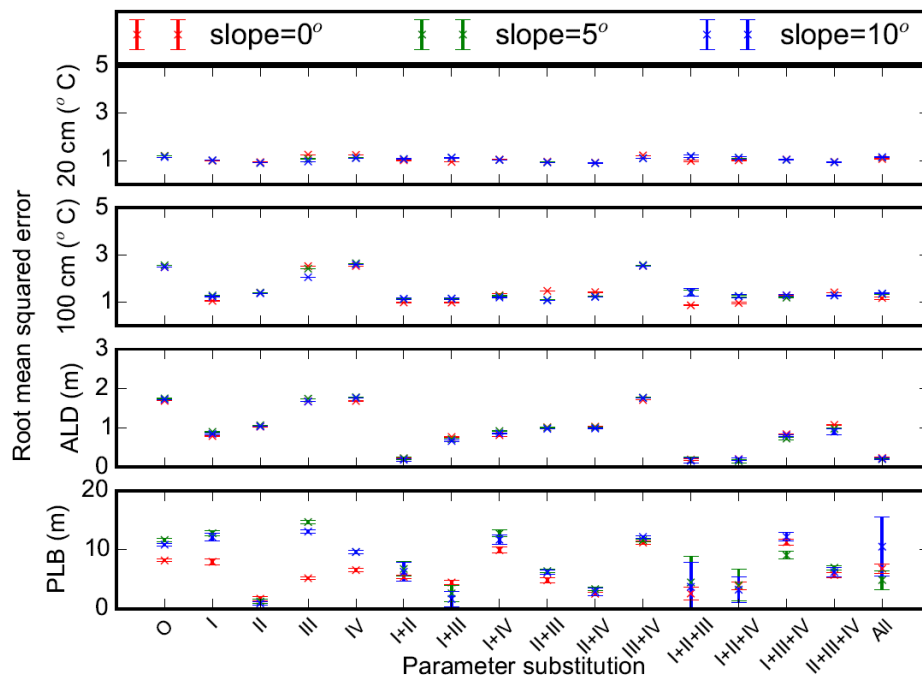
8
9
10
11
12

1 **Figure 9.** Root mean squared errors between measurements and model simulations (with
 2 different combinations of measured porosity (I), thermal conductivity (II), hydraulic
 3 conductivity (III), and matric potential (IV) of substituted for default sand parameters) for 20
 4 and 100 cm soil temperatures ($^{\circ}\text{C}$), active layer depth (ALD, m) and permafrost low
 5 boundary (PLB, m). O and All represent model runs without substitution of default
 6 parameters and with all 4 parameters substituted, respectively. Mean and standard deviation
 7 of model simulations with 3 different soil thicknesses at each slope (0° , 5° , and 10°) are shown.



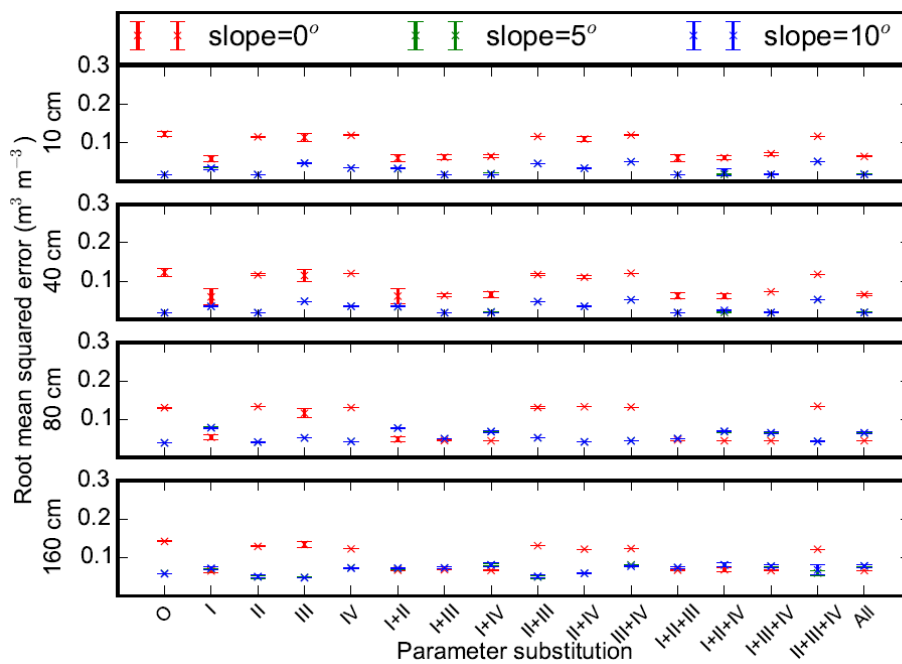
8
 9
 10

1 **Figure 10.** Root mean squared errors between measurements and model simulations (with
 2 different combinations of measured porosity (I), thermal conductivity (II), hydraulic
 3 conductivity (III) and matric potential (IV) of substituted for default loam parameters) for
 4 20 and 100 cm soil temperatures ($^{\circ}\text{C}$), active layer depth (ALD, m) and permafrost low
 5 boundary (PLB, m). O and All represent model runs without substitution of default
 6 parameters and with all 4 parameters substituted, respectively. Mean and standard deviation
 7 of model simulations with 3 different soil thicknesses at each slope (0° , 5° , and 10°) are shown.



8
 9
 10
 11
 12
 13

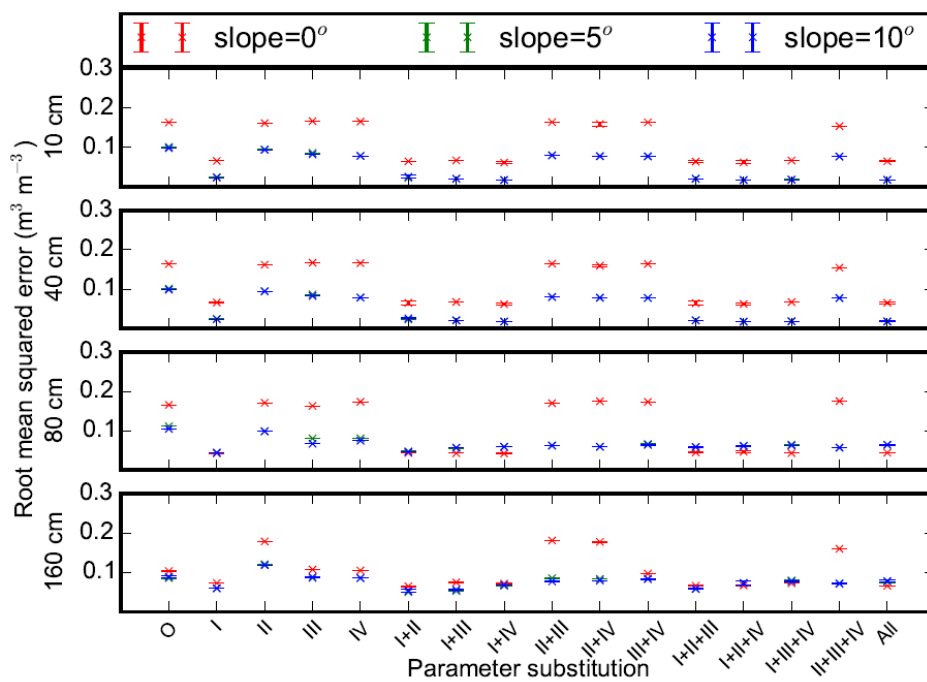
1 **Figure 11.** Root mean squared errors between measurements and model simulations (with
 2 different combinations of measured porosity (I), thermal conductivity (II), hydraulic
 3 conductivity (III), and matric potential (IV) of substituted for default sand parameters) for 10
 4 cm, 40 cm, 80 cm, and 160 cm soil volumetric liquid water content. O and All represent
 5 model runs without substitution of default parameters and with all 4 parameters substituted,
 6 respectively. Mean and standard deviation of model simulations with 3 different soil
 7 thicknesses at each slope (0° , 5° , and 10°) are shown.



8
9
10

1 **Figure 12.** Root mean squared errors between measurements and model simulations (with
 2 different combinations of measured porosity (I), thermal conductivity (II), hydraulic
 3 conductivity (III) and matric potential (IV) of substituted for default loam parameters) for
 4 10 cm, 40 cm, 80 cm and 160 cm soil volumetric liquid water content. O and All represent
 5 model runs without substitution of default parameters and with all 4 parameters substituted,
 6 respectively. Mean and standard deviation of model simulations with 3 different soil
 7 thicknesses at each slope (0° , 5° , and 10°) are shown.

8



9

10